SOCIETY OF ACTUARIES

Mitigating Extreme Risks Through Securitization

March 2017

Mitigating Extreme Risk Through Securitization

AUTHOR Jose H. Blanchet, Ph.D.
Henry Lam, Ph.D.
Qihe Tang, Ph.D.
Zhongyi Yuan, ASA, Ph.D.

SPONSOR Research Expanding Boundaries Pool

Mitigating Extreme Risks through Securitization

Jose H. Blanchet[a], Henry Lam[b], Qihe Tang[c], and Zhongyi Yuan[d]

[a]Industrial Engineering and Operations Research, Columbia University, New York, NY, USA

[b]Department of Industrial and Operations Engineering, University of Michigan, Ann Arbor, MI, USA

[c]Department of Statistics and Actuarial Science, University of Iowa, Iowa City, IA, USA

[d]Department of Risk Management, The Pennsylvania State University, University Park, PA, USA

Abstract

Due to great concerns caused by losses from catastrophes, insurers have been seeking solutions to mitigating catastrophe risks. Traditional reinsurance, despite being a commonly used solution, does not have enough capacity to digest all the catastrophe risks. Alternative risk transfer to the capital market through securitization has emerged as another solution. This report discusses securitized (re)insurance products, that is, insurance linked securities (ILSs), such as catastrophe (CAT) bonds and industry loss warranties (ILWs). Our focus is on the pricing of ILSs, as well as possible issues with using them as hedging tools, such as hedging effectiveness and basis risk. We establish a general pricing theory using CAT bonds as an example, and we establish a framework for quantifying the basis risk of hedging using ILWs as an example. In doing so, we propose to use extreme value theory to characterize the catastrophe risks involved.

1 Introduction

1.1 Catastrophe losses

Immense losses from the catastrophes that occurred in recent years have caught much attention from insurers, regulators, and academics. The year 2015 represents a typical example of such loss experience, with an overall loss of $90 billion and an insured loss of $27 billion resulting from 1,060 documented loss events worldwide, along with 23,000 fatalities, according to Munich Re[1]. At the top of the list of those causing the greatest overall losses are the Nepal earthquake in April 2015, the China/Philippines Typhoon Mujigae in October 2015, and the U.S. windstorm in February 2015, which resulted in overall losses of $4.8 billion, $3.5 billion, and $2.8 billion, respectively. At the top of those causing the greatest insured losses are the U.S. windstorm in February 2015 and the U.S. severe storms in May 2015 and in April 2015, which resulted in insured losses of $2.8 billion, $2.5 billion, and $1.6 billion, respectively. The three deadliest events are the Nepal earthquake in April 2015, the India/Pakistan heat wave in May–June 2015, and the Europe heat wave in June–August 2015, which took 9,000, 3,670, and 1,250 lives, respectively. Despite being the lowest since 2009, the 2015 loss numbers are still disconcertingly high.

[1]For details, see `https://www.munichre.com/en/media-relations/publications/press-releases/2016/2016-01-04-press-release/index.html`.

Historically, the top-five costliest catastrophes since 1980—Hurricane Katrina in 2005, the Japan earthquake in 2011, Hurricane Sandy in 2012, Hurricane Ike in 2008, and Hurricane Andrew in 1992—have cost insurers \$62 billion, \$40 billion, \$29.5 billion, \$18.5 billion, and \$17 billion, respectively [2].

Concerned with great losses, insurers are constantly seeking solutions to managing such catastrophe risks. Traditional reinsurance has been a commonly used solution, yet traditional reinsurance industry has a capacity that is too limited to digest all the catastrophe risks. An alternative solution is to securitize the risks and use insurance-linked securities (ILSs) to transfer the risks to the capital market. In view of the large size of the capital market, such an alternative risk transfer (ART) mechanism can greatly enhance the risk bearing capacity.

The focus of our report will be on ILSs and, in particular, on catastrophe (CAT) bonds and industry loss warranties (ILWs). We shall discuss the pricing of ILSs as well as possible issues with using them as hedging tools. We shall establish a general pricing theory using CAT bonds as an example, and we establish a framework for quantifying the basis risk of hedging using ILWs as an example. In doing so, we rely on extreme value theory (EVT) to model and measure the catastrophe risks involved.

1.2 Insurance-linked securities

Insurance-linked securities are financial securities that have a payoff linked to insurance risks and are often designed to provide additional funds for insurers/reinsurers to pay large claims when triggered. They have been widely used by insurers/reinsurers as a tool to transfer (catastrophic) insurance risks to the capital market. The use of ILSs helps insurers/reinsurers raise risk capital from the capital market and greatly enhances their risk-bearing capacity. Currently, commonly used ILSs in the market include CAT bonds, ILWs, and sidecars.

From ILS investors' point of view, since ILS triggering events are believed to be usually uncorrelated with the financial market (see, e.g., Lane and Beckwith 2009 and Galeotti et al. 2013), ILSs are considered as an effective diversification of their portfolio that bears an attractive yield. This has provided a sufficient demand to fuel the ILS market expansion in the current low-interest environment. The first quick expansion of the ILS market took place in 2005 after Hurricane Katrina. Although it cooled because of the 2008 financial crisis, the market regained momentum in recent years. Outstanding ILS capital has been increasing steadily from \$14.4 billion in 2011 to \$25.3 billion, \$26.0 billion, and \$26.8 billion in 2014, 2015, and 2016, respectively. In addition, the new issuances in these three years, \$9.1 billion, \$7.9 billion, and \$7.1 billion, were much higher than the new issuance of \$2.8 billion in 2008.

[2] See the page "Significant Natural Catastrophes" under "NatCatSERVICE" at `https://www.munichre.com/touch/naturalhazards/en/homepage/index.html`.

Moreover, although most ILSs are available only to sophisticated investors, the secondary market has seen a rapid growth; for example, the ILS trade volume in the first quarter of 2016 was over 25% more than that in the last quarter of 2015 (Aon Benfield)[3]. Another reason for the success of the ILS market is the large size of the capital market compared to the insurance market; a huge insurance loss of billions of dollars may be imperceptible if positioned in the U.S. bond market, which has an outstanding market of tens of trillions of dollars. This makes catastrophic insurance losses easily absorbable and has partly fueled the supply side of the ILS market. Meanwhile, the recognition of contingent capital as eligible risk capital by regulation frameworks, such as the Solvency II Directive and the Swiss Solvency Test, has also stimulated ILS supply. As of the end of 2016, the ILS outstanding risk capital is $26.8 billion, of which the majority is from CAT bonds. Therefore, we shall base most of our discussions on CAT bonds.

1.3 CAT bonds

The mechanism of CAT bonds

CAT bonds are issued by a collateralized special purpose vehicle (SPV), usually established offshore by a sponsor that is an insurer/reinsurer. The formation of the SPV helps isolate the particular catastrophe risks involved in the CAT bond investment from the sponsor's other business risks and provides investors with a pure trade of the catastrophe risks. The SPV receives premia from the sponsor and provides reinsurance coverage in return. The premia are usually paid to bond investors as part of coupon payments, which typically also contain a floating portion. The floating portion is linked to a certain reference rate such as the London Inter-Bank Offered Rate (LIBOR), reflecting the return from the trust account where the principal is deposited. When the specified catastrophic event occurs at a strength that is enough to trigger the bond, the principal and, hence, the floating portion of the coupon payments may be reduced so that some funds can be sent to the sponsor as a reimbursement for the claims paid. Usually offered with a maturity of one to five years, CAT bonds have the advantage of providing insurers/reinsurers with coverage for multiple years without incurring extra transaction costs. See Cummins (2008) for related discussions.

The choice of trigger

In the design of CAT bonds, of great importance is the choice of trigger, which can be categorized into indemnity triggers and nonindemnity triggers. Indemnity triggers trigger the bond according to the sponsor's actual loss due to the specified catastrophic events, while in contrast, nonindemnity triggers are based on other quantities chosen to reflect/approximate (yet unlikely to precisely represent) the actual loss. Typical nonindemnity triggers include industry loss triggers, parameter

[3] See http://ir.aon.com/about-aon/investor-relations/investor-news/news-release-details/2016/Catastrophe-bond-issuance-set-first-quarter-record-of-22bn-according-to-Aon-ILS-study/default.aspx.

triggers, modeled loss triggers, and hybrid triggers. Industry loss triggers trigger the bond when the value of a chosen industry loss index, such as the Property Claims Services (PCS) index, exceeds some threshold. Parameter triggers trigger the bond when a parameter of the catastrophic event exceeds some threshold, such as the magnitude of an earthquake being measured over 7.0 or the Chicago Mercantile Exchange Hurricane Index exceeding 10.0. Modeled loss triggers trigger the bond based on the loss calculated via a model provided by a recognized agency such as Applied Insurance Research Worldwide, EQECAT, and Risk Management Solutions. Hybrid triggers combine the above-mentioned triggers and can be useful for bonds that cover multiple perils. We refer the reader to Dubinsky and Laster (2003), Guy Carpenter & Company (2007), and Cummins (2008) for related discussions of the triggers.

Among the five types of triggers, the most popular ones are indemnity triggers and industry loss index triggers. As of the end of 2016, about 63.9% of CAT bond and other ILS outstanding risk capital is based on an indemnity trigger, and about 24.7% is based on an industry loss index trigger[4]. There is a trend that indemnity-triggered bonds are taking a higher proportion. According to Cummins and Weiss (2009), the most popular CAT bond triggers during 1997–2007 were indemnity triggers, parameters triggers, and industry index triggers, which took up 30%, 25.9%, and 21.5%, respectively.

The choice of trigger is essentially a trade-off between moral hazard and basis risk. Indemnity triggers are known to provide a better hedge for the sponsor since the resulted claim reimbursement is perfectly linked to the sponsor's loss, leading to lower basis risk. However, the use of indemnity triggers involves disadvantages such as bond investors' concern with moral hazard in the calculation of the sponsor's loss and the sponsor's concern with confidential information disclosure. Also, due to the long loss adjustment process, indemnity-triggered bonds usually take a much longer time to settle than some nonindemnity-triggered bonds (e.g., parameter-triggered bonds). Therefore, investors demand a higher yield from indemnity-triggered bonds, a phenomenon suggested by Dubinsky and Laster (2003) and Cummins and Weiss (2009) and empirically verified by Galeotti et al. (2013). With nonindemnity triggers moral hazard can be significantly reduced. However, due to possible lack of dependence between the nonindemnity trigger of choice and the sponsor's loss, there could be substantial basis risk that the CAT bond cannot effectively hedge the sponsor's loss.

Examples of CAT bonds

Here we list three examples of CAT bonds[5] issued in the past to show some typical designs.

Example 1.1 Kamp Re 2005 Ltd.

- Issuer: Kamp Re 2005 Ltd.

[4]See `http://www.artemis.bm/deal_directory/cat_bonds_ils_by_trigger.html`.

[5]Details of these bonds can be found at `http://www.artemis.bm`.

- Sponsor: Swiss Reinsurance America Corp.
- Catastrophe risks covered: U.S. hurricane and U.S. earthquake
- Issue date: August 2005
- Maturity date: August 2008
- Amount: $190 million
- Ratings: BB+ (Standard & Poor's)
- Trigger type: Indemnity (triggered if losses from one single hurricane or earthquake exceeds $1 billion)

Kamp Re 2005 Ltd. was the first natural CAT bond triggered, and investors lost 75% of the principal. This had a substantial impact on the prices of CAT bonds issued afterwards.

Example 1.2 Muteki Ltd.

- Issuer: Muteki Ltd. Cedent
- Sponsor: Zenkyoren
- Catastrophe risk covered: Japan earthquake
- Issue date: May 2008
- Maturity date: May 2011
- Amount: $300 million
- Ratings: Ba2 (Moody's)
- Trigger type: Parametric

Because of the March 11, 2011, Japan earthquake, the bond was triggered about 10 weeks before maturity. The investors lost all of the $300 million principal.

Example 1.3 Acorn Re Ltd. (Series 2015-1)

- Issuer: Acorn Re Ltd.
- Sponsor: Hannover Rück SE / Oak Tree Assurance, Ltd.
- Catastrophe risks covered: U.S. earthquake
- Issue date: July 2015
- Maturity date: July 2018
- Amount: $300 million
- Ratings: BBsf (Fitch)
- Trigger type: Parametric

We shall use this bond as a prototype when discussing CAT bond pricing in Section 4.1.

The first two examples show cases where some (or all) bond principal is lost because of the occurrence of the specified catastrophic events. It is noteworthy that, although CAT bonds are designed to provide investors with a pure trade of insurance risk and to eliminate credit risk via collateral accounts, the flaws of the Total Return Swap structure that prevailed before the 2008 financial crisis have caused principal losses for investors. In fact, four of the 10 principal losses (the 2006 deal issued by Carillon Ltd., the 2007 deal issued by Ajax Re Ltd., and the 2008 deals issued by Newton Re and Willow Re) are due to the failure of Lehmann Brothers, who acted as the swap counterparty; see NAIC (2012). Since then much improvement has been made on the collateral structure to further reduce credit risk.

1.4 Industry loss warranties

ILWs are a kind of reinsurance contract that reimburses the purchaser when triggered. Typically used triggers include indemnity triggers and index loss triggers. Dual-triggered ILW contracts have both an indemnity trigger and an index loss trigger; that is, such contracts are triggered when both the company specific loss is beyond some limit and the industry loss as a whole is also over some attachment point. Compared to traditional reinsurance, index-triggered ILWs are highly standardized, have relatively low transaction costs, are less susceptible to moral hazard, and are more liquidly traded in the secondary market. They can be offered both before and after the occurrence of perils (although it must be before the estimated industry loss is publicly available). Although some of the features may become less prominent after the introduction of an indemnity trigger to the ILW contract, the indemnity trigger generally makes the contract look friendlier to regulators. The purchase of ILWs with an indemnity trigger is considered as a reinsurance purchase by regulators and will help reduce the insurer or reinsurer's required risk capital.

ILWs also take up a significant portion of the ILS market and have been serving as another solution to catastrophe risk transfer. The size of the ILW market used to be approximately of the same order as that of the CAT bond market (Cummins 2008), although it appears not to be growing as fast. Because of the lack of data, a precise and most updated estimate of the size is not available[6].

To understand a typical design of ILW, below we show a hypothetical example, excerpted from McDonnell (2002):

- Term: 01/01/2014–12/31/2014
- Territory: 48 U.S. states
- Perils covered: all natural catastrophes
- Index: PCS
- Industry loss trigger: $10 billion
- Company loss trigger: $100 million
- Coverage limit: $300 million
- Reporting period: 36 months

[6] See `http://www.willisre.com/documents/Media_Room/Publication/Willis_Re_Q1_2012_ILW.pdf` for a summary of the market size until 2012.

- Premium: 12% (rate-on-line) of coverage limit

The rest of this report contains five sections. Section 2 introduces EVT and prepares the theoretical framework that will be used for modeling extreme risks and their extreme dependence. Section 3 proposes a general pricing framework using a product pricing measure. Section 4 illustrates the pricing framework as well as the use of EVT using two CAT bonds as examples. Section 5 discusses the basis risk of ILWs for both ILWs with average-sized attachment points and ILWs with large attachment points. Finally, Section 6 collects technical proofs and details of the interest rate models used throughout the report.

2 Modeling Extreme Risks

Apparently, both the pricing of such ILSs and the quantification of their basis risk will have to rely on proper modeling of the underlying extreme risks and their extreme dependence. In this section, we prepare a few general modeling frameworks that are useful for these purposes.

2.1 Modeling extreme dependence

Since aggregate insurance losses are often modeled by sums of (dependent) random variables, we pay special attention to such sum structures. Assume that the losses from d individual events or d covered regions are X_1, …, X_d and, hence, the aggregate amount of losses is

$$S_d = \sum_{j=1}^{d} X_j.$$

While there are well-established statistical methods available for characterizing the marginal distributions of the losses $X_1, \ldots, X_d$, it is in general much harder to model the intangible dependence structures among them.

Since we are concerned with extreme risks, we focus on dependence in the tail area, which we shall interchangeably call tail dependence, extreme dependence, or asymptotic dependence. Two random variables Y_1 and Y_2 with distribution functions G_1 and G_2 are said to be tail dependent if they have a significant tendency of extreme comovement, that is, if their coefficient of upper tail dependence, defined by

$$\lim_{u \uparrow 1} P\left(G_1(Y_1) > u | G_2(Y_2) > u\right),$$

exists and is positive. The coefficient of lower tail dependence can be defined in a similar way.

The characterization of tail dependence is of great importance in modeling extreme risks. We propose a risk factor approach to this problem. Generally, one may assume that the individual losses $X_1, \ldots, X_d$ are exposed to a common risk factor θ, which can be either univariate or multivariate depending on a given situation. This risk factor summarizes the impacts of various intrinsic quantities of interest and plays an important role in modeling tail dependence. For example, in earthquake insurance the risk factor θ can be chosen to be the earthquake magnitude, in agricultural insurance it can be weather indices such as the temperature and precipitation, in health insurance it can be the spread of a pandemic and the effect of a corresponding vaccine, and in life insurance it can be some environmental factor that influences the mortality rate. If financial investments are considered, then θ can be represented by some underlying macroeconomic factors. Usually, this risk factor θ is crucial in affecting the strength of tail dependence. A flexible model therefore ought to span a wide range of tail dependence when θ varies.

Among many models for dependence structures, copula models are particularly useful. A copula with dimension d is a joint distribution function of d uniform $(0,1)$ random variables. For individual losses $X_1, \ldots, X_d$ with specified marginal distributions $F_1, \ldots, F_d$, one can incorporate a copula, denoted by $C(\mathbf{u})$ for $\mathbf{u} \in (0,1)^d$, to model their dependence. We say that the random vector $\mathbf{X} = (X_1, \ldots, X_d)$ has a copula C if it holds for every $\mathbf{x} \in \mathbb{R}^d$ that

$$P\left(X_1 \leq x_1, \ldots, X_d \leq x_d\right) = C(F_1(x_1), \ldots, F_d(x_d)).$$

See, for example, Nelsen (2006) for a comprehensive treatment of copulas.

To capture the tail dependence among insurance losses, one may consider t-copulas. To specify a t-copula, one needs a degree of freedom v and a positive definite correlation matrix $\varrho = (\rho_{jk})$. Then the t-copula is given by

$$C^t_{v,\varrho}(\mathbf{u}) = \mathbf{t}_{v,\varrho}\left(t_v^{-1}(u_1), \ldots, t_v^{-1}(u_d)\right), \qquad \mathbf{u} \in (0,1)^d,$$

where $\mathbf{t}_{v,\varrho}$ is the joint distribution function of a d-dimensional t distribution with degree of freedom v, mean $\mathbf{0}$, and correlation matrix ϱ, and t_v^{-1} is the quantile function of a standard univariate t distribution with degree of freedom v. In the risk factor approach, a risk factor θ can be put into the correlation matrix in the copula and can be calibrated from data.

Other copula choices can model tail dependence, each having its own merits and demerits. For example, t-copulas, while being able to depict tail dependence, have upper and lower tails that behave very similarly. More precisely, if the random vector $\mathbf{X}$ possesses a t-copula, then every pair of its components has the same coefficient of upper and lower tail dependence; see, for example, Section 7.3.1 of McNeil et al. (2015). Hence, t-copulas do not have the flexibility to model different upper and lower tail dependence structures. On the other hand, Gumbel copulas, given by

$$C(\mathbf{u}) = \exp\left\{-\left(\sum_{j=1}^{d}(-\ln u_j)^{\gamma}\right)^{1/\gamma}\right\}, \qquad \mathbf{u} \in (0,1)^d,\ 1 \leq \gamma \leq \infty, \tag{2.1}$$

potentially resolve this issue and can be another good candidate for modeling tail dependence. An important feature of Gumbel copulas is that the pairwise coefficient of lower tail dependence is 0 while the pairwise coefficient of upper tail dependence is $2 - 2^{1/\gamma}$, which is positive if $\gamma > 1$. It is easy to see that letting $\gamma = 1$ in (2.1) results in the independence copula

$$C_{\text{ind}}(\mathbf{u}) = \prod_{i=1}^{d} u_i,$$

while letting $\gamma = \infty$ results in the comonotonicity copula

$$C_{\text{com}}(\mathbf{u}) = \min_{1 \le i \le d} u_i.$$

Concerning the risk factor approach, if we link the parameter γ of a Gumbel copula to a risk factor θ in a suitable way, then we can span the range of tail dependence from asymptotic independence to asymptotic full dependence, as θ varies from its normal range to its extrema.

2.2 Extreme value distributions

It is natural to consider using an asymptotic method for tail risk analysis. Asymptotically, one may use extreme value distributions to approximate the distributions of certain quantities of interest, such as the maximum loss within a period of time and the exceedance of loss over a high threshold.

Specifically, for a distribution function F, let M_n be the maximum of a sample of size n from F. If there are normalizing constants $c_n > 0$ and $d_n \in \mathbb{R}$ such that $c_n^{-1}(M_n - d_n)$ converges weakly to a nondegenerate distribution H, then we say that F belongs to the max-domain of attraction (MDA) of H. By the well-known Fisher–Tippett–Gnedenko theorem, H must be a member of the family of generalized extreme value distributions whose standard version is

$$H_\xi(x) = \exp\left\{-(1+\xi x)^{-1/\xi}\right\}, \qquad 1 + \xi x > 0,$$

where $(1+\xi x)^{-1/\xi}$ is interpreted as e^{-x} for $\xi = 0$. This unifies the three extreme value types: Fréchet, Gumbel, and Weibull.

Moreover, the well-known one-dimensional peaks-over-threshold (POT) theorem states that, for $F \in \text{MDA}(H_\xi)$ with a finite or infinite upper endpoint x_F, there exists a positive function a such that, for $x > 0$ and $1 + \xi x > 0$,

$$\lim_{y \uparrow x_F} P\left(\frac{X - y}{a(y)} > x \,\middle|\, X > y\right) = (1+\xi x)^{-1/\xi}.$$

This means that the scaled excesses over a high threshold y converge weakly to the generalized Pareto distribution (GPD). The auxiliary function a, as well as the normalizing constants c_n and d_n above, can be explicitly expressed; see, for example, Theorem 1.1.6 of de Haan and Ferreira (2006). With the convergence above, approximations for the tail probability of X and some tail-related risk measures such as value at risk (VaR) and conditional tail expectation will be straightforward.

By incorporating a scale parameter the GPD above can be extended to

$$G_{\xi,\beta}(x) = 1 - \left(1 + \xi\frac{x}{\beta}\right)^{-1/\xi}, \qquad \beta > 0,$$

where $x \geq 0$ if $\xi \geq 0$ and $0 \leq x \leq -\beta/\xi$ if $\xi < 0$. As stated in Theorem 3.4.13(e) of Embrechts et al. (1997), for a random variable X following the GPD $G_{\xi,\beta}$, its mean excess function is a linear function,

$$e(y) = E\left[X - y | X > y\right] = \frac{\beta + \xi y}{1 - \xi}, \qquad \beta + \xi y > 0.$$

The linearity allows us to use a plot of the estimated mean excess function to check whether a GPD is a good fit to the data.

Details of these concepts and results are available in standard monographs of EVT such as Embrechts et al. (1997), Beirlant et al. (2004), and de Haan and Ferreira (2006). Applications of EVT to insurance, finance, and risk management can be found in Embrechts et al. (1998, 1999), McNeil and Frey (2000), Bali (2007), Zimbidis et al. (2007), Donnelly and Embrechts (2010), Kellner and Gatzert (2013), Kelly and Jiang (2014), McNeil et al. (2015), and van Oordt and Zhou (2016), among many others.

2.3 Univariate and multivariate regular variation

The modeling of tail dependence and extreme sizes of losses can be packed into a unified modeling framework using the notion of multivariate regular variation (MRV).

We start with univariate regular variation. A positive function f on $\mathbb{R}^+ = [0, \infty)$ is said to be regularly varying at ∞ with regularity index $\alpha \in \mathbb{R}$, written as $f \in \mathrm{RV}_\alpha$, if

$$\lim_{x \to \infty} \frac{f(xz)}{f(x)} = z^\alpha, \qquad z > 0.$$

Thus, $f \in \mathrm{RV}_\alpha$ if and only if

$$f(x) = x^\alpha l(x) \tag{2.2}$$

for some slowly varying function l (that is, $l \in \mathrm{RV}_0$). See Bingham et al. (1987) and Resnick (1987) for textbook treatments of regular variation.

Let X be a random variable distributed by F on $\mathbb{R}_+$ with tail $\overline{F} = 1 - F \in \mathrm{RV}_{-\alpha}$, $\alpha > 0$; that is,

$$\lim_{x \to \infty} \frac{\overline{F}(xz)}{\overline{F}(x)} = z^{-\alpha}, \qquad z > 0. \tag{2.3}$$

By relation (2.2), the tail $\overline{F}(x)$ decays roughly at a power rate. Hence, the random variable X and its distribution function F are often said to be of Pareto type. Commonly used distributions such as Pareto, Student's t, F, Burr, Loggamma, Fréchet, and inverse gamma distributions are all of the Pareto type. Note that a Pareto-type distribution is heavy tailed in the sense that its right tail is heavier than that of any exponential distribution.

An MRV structure can be used to model both extreme losses and their extreme dependence. For illustration, we consider a simple case where all marginal distributions of the losses have tails equivalent to that of a Pareto-like distribution function F. Denote the space $[0, \infty]^d$ by $[\mathbf{0}, \boldsymbol{\infty}]$. A random vector $\mathbf{X} = (X_1, \ldots, X_d)$ is said to possess an MRV structure on $[\mathbf{0}, \boldsymbol{\infty}]\backslash\{\mathbf{0}\}$ if there exists a limit measure ν on $[\mathbf{0}, \boldsymbol{\infty}]\backslash\{\mathbf{0}\}$, not identically 0, such that, for every $\mathbf{z} > \mathbf{0}$,

$$\lim_{x\to\infty} \frac{1}{\overline{F}(x)} P\left(\frac{\mathbf{X}}{x} \in [\mathbf{0}, \mathbf{z}]^c\right) = \nu\left([\mathbf{0}, \mathbf{z}]^c\right), \tag{2.4}$$

where $[\mathbf{0}, \mathbf{z}]^c$ is the complement of the set $[\mathbf{0}, \mathbf{z}]$. Note that the MRV structure is indeed a multivariate extension of univariate regular variation. On the one hand, the univariate regular variation described by (2.3) corresponds to (2.4) with $d = 1$ and $\nu\left([0, z]^c\right) = z^{-\alpha}$; on the other hand, the multivariate regular variation described by (2.4) implies that some, and maybe all, marginal tails of $\mathbf{X}$ are regularly varying. For detailed discussions of MRV, we refer the reader to the monographs by de Haan and Ferreira (2006) and Resnick (2007).

This structure provides us with great generality for modeling, in the sense that all random vectors with Pareto-like marginal distributions will follow this structure as long as the dependence among their components satisfies some mild conditions. Such dependence can be produced by, for instance, mixtures and various copulas such as Gaussian, t, and Archimedean copulas; see, for example, Li and Sun (2009) and Tang and Yuan (2013). Dependence in the tail of particular strength can be captured through a particular limit measure ν. For example, strong tail dependence, which could give rise to joint large losses, can be captured by a limit measure that assigns mass to the interior area $(\mathbf{1}, \boldsymbol{\infty}]$, while weak tail dependence can be modeled by a limit measure concentrated on the axes only. Indeed, if $\nu((\mathbf{1}, \boldsymbol{\infty}]) > 0$, then for $d \geq 2$ we have, for example,

$$\lim_{x\to\infty} \frac{P(X_1 > x, X_2 > x)}{P(X_1 > x)} = \frac{\nu\left((1,\infty] \times (1,\infty] \times [0,\infty]^{d-2}\right)}{\nu\left((1,\infty] \times [0,\infty]^{d-1}\right)} > 0.$$

This together with the tail equivalence of the marginal distribution functions implies that X_1 and X_2 are tail dependent.

Below we show a few examples where an MRV structure naturally arises from various specifications; they also show how the strength of tail dependence is reflected by the limit measure.

Example 2.1 Suppose that X_1, ..., X_d are independent, identically distributed (i.i.d.) following a common Pareto distribution with shape and scale parameters α and θ_F:

$$F_1(x) = \cdots = F_d(x) = F(x) = 1 - \left(\frac{\theta_F}{x + \theta_F}\right)^{\alpha}, \qquad x > 0. \tag{2.5}$$

Then for every $\mathbf{z} > \mathbf{0}$,

$$\begin{aligned} \lim_{x\to\infty} \frac{1}{\overline{F}(x)} P\left(\frac{\mathbf{X}}{x} \in [\mathbf{0}, \mathbf{z}]^c\right) &= \lim_{x\to\infty} \frac{1}{\overline{F}(x)} P\left(\bigcup_{j=1}^{d} \left(\frac{X_j}{x} > z_j\right)\right) \\ &= \lim_{x\to\infty} \frac{1}{\overline{F}(x)} \sum_{j=1}^{d} P\left(X_j > xz_j\right) = \sum_{j=1}^{d} z_j^{-\alpha}. \end{aligned}$$

Therefore, we see that $\mathbf{X}$ possesses an MRV structure, and relation (2.4) holds with ν defined by

$$\nu\left([\mathbf{0},\mathbf{z}]^c\right)=\sum_{j=1}^d z_j^{-\alpha},\qquad \mathbf{z}>\mathbf{0}.$$

Here the limit measure ν is concentrated on the axes only. Precisely, it assigns a mass of $z^{-\alpha}$ to the interval $[z,\infty]$ on each axis for any $z>0$.

Example 2.2 Suppose that X_1, …, X_d are identically distributed by F, a t distribution with degree of freedom v. Also suppose that $\mathbf{X}$ has a Gaussian copula C given by

$$C\left(u_1,\ldots,u_d\right)=\Phi_d\left(\Phi^{-1}\left(u_1\right),\ldots,\Phi^{-1}\left(u_d\right);\Sigma\right),\qquad \mathbf{u}\in[0,1]^d,$$

where Φ_d is a d-dimensional standard normal distribution function with correlation matrix $\Sigma=\left(\rho_{ij}\right)_{1\le i,j\le d}$, and Φ is the univariate standard normal distribution function. Then $\mathbf{X}^+=(X_1\vee 0,\ldots,X_d\vee 0)$ possesses an MRV structure and relation (2.4) holds with ν defined by

$$\nu\left([\mathbf{0},\mathbf{z}]^c\right)=\sum_{\emptyset\neq I\subseteq\{1,\ldots,d\}}(-1)^{|I|-1}\left(\min_{i\in I} z_i^{-\alpha}\right)1_{\left(\rho_{jk}=1\text{ for }j,k\in I\right)},\qquad \mathbf{z}>\mathbf{0};$$

see Lemma 6.4 of Yuan (2016). In the case that $\rho_{jk}<1$ for all $1\le j<k\le d$, the components of $\mathbf{X}^+$ are asymptotically independent, and the limit measure ν, just like in Example 2.1, is concentrated on the axes and assigns a mass of $z^{-\alpha}$ to the interval $[z,\infty]$ on each axis for any $z>0$. Note that this leads to a situation where we cannot distinguish asymptotic independence from complete independence by solely specifying the limit measure. By contrast, if $\rho_{jk}=1$ for some $1\le j<k\le d$, that is, if X_j and X_k have a total positive linear relationship, then X_j and X_k are comonotonic (i.e., they have the comonotonicity copula) and ν is concentrated on the hyperplane $\{\mathbf{z}\in[\mathbf{0},\boldsymbol{\infty}]:z_j=z_k\}$.

Example 2.3 Suppose that X_1, …, X_d all follow the Pareto distribution given by (2.5). In addition, suppose that $\mathbf{X}$ has a Gumbel copula of form (2.1). Then, by Lemma 5.2 of Tang and Yuan (2013), $\mathbf{X}$ possesses an MRV structure and relation (2.4) holds with ν defined by

$$\nu\left([\mathbf{0},\mathbf{z}]^c\right)=\left(\sum_{j=1}^d z_j^{-\alpha\gamma}\right)^{1/\gamma},\qquad \mathbf{z}>\mathbf{0}.$$

If $\gamma=1$, the limit measure ν is still concentrated on the axes and assigns a mass of $z^{-\alpha}$ to the interval $[z,\infty]$ on each axis for any $z>0$. By contrast, if $\gamma>1$, then ν assigns positive mass to the interior $(\mathbf{0},\boldsymbol{\infty}]$, leading to asymptotic dependence among X_1, …, X_d. In particular, if $\gamma=\infty$, then ν is concentrated on the diagonal $\{\mathbf{z}\in[\mathbf{0},\boldsymbol{\infty}]:z_1=\cdots=z_d\}$.

It is easy to extend Examples 2.1–2.3 to the case where the marginal distributions are nonidentical Pareto with the same or even different shape parameters while the loss vector $\mathbf{X}$ still possesses an MRV structure with the limit measure ν explicitly given. To keep the report short, we do not expand this discussion here, but we would like to point out that such extensions are important when dealing with inhomogeneous insurance portfolios.

One more advantage of the MRV framework is its nonparametric nature in characterizing tail dependence, which makes it less susceptible to model misspecification. Note that such a model misspecification issue is always a concern while using copula-based models; for example, one may mistakenly specify a t-copula model for data generated from a Gumbel copula.

Moreover, in extreme risk management one often needs to estimate the probability that losses become jointly large or fall into some high-risk region. While the estimation is relatively easy by our method when tail dependence is present, it becomes harder when losses are asymptotically independent, because in this situation the event becomes less discernible and the target probability becomes even smaller. For this case, it is helpful to characterize the tail behavior of losses in a finer manner by the so-called hidden regular variation (HRV) structure. Such a finer characterization also becomes particularly useful in situations like Examples 2.1 and 2.2, where one cannot distinguish asymptotic independence from complete independence by just using a limit measure. We refer the reader to Resnick (2007) and Mitra and Resnick (2011) for detailed discussions of HRV.

With the above mathematical tools, we show that it is relatively easy to study the tail behavior of the aggregate loss. For simplicity, consider the case where the loss variables $X_1, \ldots, X_d$ all follow a Pareto distribution F with shape parameter $\alpha > 0$, and they jointly possess a Gumbel copula with parameter $\gamma > 1$ as given before. Then by the MRV structure presented in Example 2.3, we obtain

$$\lim_{x\to\infty} \frac{P\left(S_d > x\right)}{\overline{F}(x)} = \nu(A), \tag{2.6}$$

where $A = \{\mathbf{z} \in [\mathbf{0}, \boldsymbol{\infty}] : \sum_{j=1}^{d} z_j > 1\}$. This type of approximations can be derived under more general assumptions and can be translated seamlessly to obtain similar formulas in the case that the underlying parameter governing the strength of dependence is random and linked to a certain risk factor.

3 A General Pricing Framework

As the CAT bond market expands, the pricing of CAT bonds becomes increasingly important and has attracted much research attention. We introduce in this section a general framework for CAT bond pricing.

3.1 CAT bond terms

Consider a CAT bond with maturity date T and principal/face value K. The bond makes annual coupon payments to investors at the end of each year for T years and makes a final redemption payment on the maturity date T. The coupons are structured to contain two parts: (1) a fixed part as the premium paid to bond investors for the reinsurance coverage and (2) a floating part equal to the return, at the LIBOR, on the bond sale proceeds that are deposited in a trust.

Suppose that the coupon payments and final redemption are linked to the occurrence of the specified natural catastrophes and financial catastrophes. It is worthwhile mentioning that events such as the default of the trustee and massive mortgage defaults could be sources of catastrophic financial risks. Trustee defaults have occurred in the past; see, for example, NAIC (2012). There are also recent CAT bond issuances that covered catastrophic financial risks; the one issued by Bellemeade Re Ltd. in July 2015 that covered mortgage default risk is an example[7]. Thus, we aim to propose a framework general enough to include two triggers: (1) an indemnity/nonindemnity insurance risk trigger Y, based on the occurrence of the specified natural catastrophes, and (2) a financial risk trigger Z, based on the occurrence of the specified financial catastrophes. If the bond is triggered, part or even all of the principal is liquidated from the collateral to reimburse the sponsor's claim losses, and the floating coupon is reduced according to the amount of principal remaining; otherwise, the bond just behaves like a default-free coupon bond.

We model the insurance risk trigger Y to be a non-negative, nondecreasing, and right-continuous stochastic process $\{Y_t, t \geq 0\}$ defined on a filtered physical probability space $(\Omega^1, \mathcal{F}^1, \{\mathcal{F}_t^1\}, P^1)$. In the context of earthquake CAT bonds, an example of the insurance risk trigger process $\{Y_t, t \geq 0\}$ is the maximum magnitude of earthquakes, or the number of earthquakes with magnitude above a certain threshold, within a certain region during $[0, t]$; see Section 4.1 for more discussion. Another example of $\{Y_t, t \geq 0\}$ is the sponsor's loss or the statewide loss from the specified catastrophic events prior to time t, which is often modeled as a compound Poisson process. In this case, the Poisson process represents the number of the specified catastrophic events, and the i.i.d. non-negative random variables, independent of the Poisson process, represent the amounts of losses incurred from individual catastrophic events. More discussion of a bond using such a trigger can be found in Section 4.2.

Similarly, the financial risk trigger Z is modeled as another non-negative, nondecreasing, and right-continuous stochastic process $\{Z_t, t \geq 0\}$ defined on a filtered physical probability space $(\Omega^2, \mathcal{F}^2, \{\mathcal{F}_t^2\}, P^2)$, on which an arbitrage-free financial market is also defined. Note here that an increase of Z usually results from a financial market decline, which exposes the insurer to higher financial risk. An example of the financial risk trigger process is the drop of a certain stock price index (e.g., the Dow Jones Industrial Average Index) if the CAT bond is designed to be triggered when the overall economy turns down. If the CAT bond is designed to cover mortgage default risk, then the running maximum of delinquency rate indices such as the S&P/Experian First Mortgage Default Index can be used as the financial risk trigger process.

[7]For details, see `http://www.artemis.bm/deal_directory/bellemeade-re-ltd-series-2015-1/`.

Given the two physical probability spaces $(\Omega^1, \mathcal{F}^1, \{\mathcal{F}^1_t\}, P^1)$ and $(\Omega^2, \mathcal{F}^2, \{\mathcal{F}^2_t\}, P^2)$, we introduce the product space $(\Omega, \mathcal{F}, \{\mathcal{F}_t\}, P)$ with $\Omega = \Omega^1 \times \Omega^2$, $\mathcal{F} = \mathcal{F}^1 \times \mathcal{F}^2$ being the smallest sigma field covering $A_1 \times A_2$ for all $A_1 \in \mathcal{F}^1$ and $A_2 \in \mathcal{F}^2$, $\mathcal{F}_t = \mathcal{F}^1_t \times \mathcal{F}^2_t$ for each fixed $t \geq 0$, and $P = P^1 \times P^2$. An implication of the expression $P = P^1 \times P^2$ is that the two probability spaces are assumed to be independent, which is reasonable in view of the low correlation between the occurrence of natural catastrophes and the performance of the financial market. Thus, under this product probability measure P, the development of the trigger is independent of the performance of the financial market.

For all random variables defined on one of the two spaces, we can easily redefine them in the product space $(\Omega, \mathcal{F})$ in a natural way. For instance, for random variables $Y^1(\omega_1)$ and $Y^2(\omega_2)$ defined on the spaces $(\Omega^1, \mathcal{F}^1)$ and $(\Omega^2, \mathcal{F}^2)$, respectively, we can extend them to be $Y^1(\omega_1, \omega_2) = Y^1(\omega_1)1_{\Omega_2}(\omega_2)$ and $Y^2(\omega_1, \omega_2) = 1_{\Omega_1}(\omega_1)Y^2(\omega_2)$, so that they are defined on the product space $(\Omega, \mathcal{F})$. Then it is easy to verify that $Y^1(\omega_1, \omega_2)$ and $Y^2(\omega_1, \omega_2)$ are independent of each other under the product measure P. Actually, for two Borel sets B_1 and B_2, we have

$$
\begin{aligned}
& P\left(Y^1(\omega_1, \omega_2) \in B_1,\ Y^2(\omega_1, \omega_2) \in B_2\right) \\
= \ & P\left(\left(Y^1(\omega_1) \in B_1\right) \times \Omega^2,\ \Omega^1 \times \left(Y^2(\omega_2) \in B_2\right)\right) \\
= \ & P^1 \times P^2 \left(\left(Y^1(\omega_1) \in B_1\right) \times \left(Y^2(\omega_2) \in B_2\right)\right) \\
= \ & P^1 \left(Y^1(\omega_1) \in B_1\right) P^2 \left(Y^2(\omega_2) \in B_2\right) \\
= \ & P\left(Y^1(\omega_1, \omega_2) \in B_1\right) P\left(Y^2(\omega_1, \omega_2) \in B_2\right).
\end{aligned}
$$

See Section 5 of Cox and Pedersen (2000) for similar discussions. In what follows, we always tacitly follow this interpretation when we have to extend random variables defined on the two individual spaces to the product space.

The remaining principal of the CAT bond at time t depends on the developments of the insurance risk trigger Y and the financial risk trigger Z over $[0, t]$. To quantify this, we introduce a bivariate function $\Pi(\cdot, \cdot) : [0, \infty) \times [0, \infty) \to [0, 1]$, component-wise nonincreasing and right-continuous with $\Pi(0, 0) = 1$, such that the remaining principal of the CAT bond at any time $t \in [0, T]$ is equal to

$$K\Pi\left(Y_t, Z_t\right).$$

In particular, the remaining principal at maturity is equal to $K\Pi\left(Y_T, Z_T\right)$. Note that we do not exclude the possibilities of $\Pi(y, \infty)$, $\Pi(\infty, z)$, or $\Pi(\infty, \infty)$ being positive, which mean that even in extreme scenarios the bond investors may still get back some principal. Moreover, the occurrence of a natural and/or financial catastrophe at time t wipes off an amount equal to

$$K\Pi\left(Y_{t-0}, Z_{t-0}\right) - K\Pi\left(Y_t, Z_t\right)$$

from the principal. As we see, by stipulating a plan of allocating the principal between the investor and the sponsor according to the developments of triggers Y and Z, this bivariate function $\Pi(\cdot,\cdot)$ plays a crucial role in the CAT bond's construction.

As time passes, while the fixed part of the coupon payments (i.e., the premium payments) remains unchanged, the floating part may be reduced due to the reduction in principal. More precisely, let the fixed annual coupon rate be R, let the floating annual coupon rate be i_t over year t (i.e., from time $t-1$ to time t), $t = 1, \dots, T$, and let r_t be the annualized instantaneous risk-free interest rate at t, $t \geq 0$, where the stochastic processes $\{i_t, t = 1, \dots, T\}$ and $\{r_t, t \geq 0\}$ are defined on $(\Omega^2, \mathcal{F}^2)$. Therefore, on each coupon payment date, the bond investor receives

$$KR + Ki_t\Pi\left(Y_{t-1}, Z_{t-1}\right), \qquad t = 1, \dots, T.$$

With a pricing measure Q, which we shall determine in Section 3.2, the price at time $t \in [0, T]$ of the CAT bond is given by

$$P_t = KE^Q\left[\sum_{s=\lfloor t \rfloor+1}^{T} D(t,s)\left(R + i_s\Pi\left(Y_{s-1}, Z_{s-1}\right)\right) + D(t,T)\Pi\left(Y_T, Z_T\right)\middle| \mathcal{F}_t^1 \times \mathcal{F}_t^2\right], \qquad (3.1)$$

where $\lfloor t \rfloor$ denotes the integer part of t and $D(t,s) = \exp\left\{-\int_t^s r_u\,du\right\}$ denotes the corresponding discount factor over the interval $[t,s]$. As it shows, in the case where t is exactly a coupon date, formula (3.1) gives the price immediately after this coupon payment is made. Hereafter, we use $E_t^Q[\cdot] = E^Q\left[\cdot\middle| \mathcal{F}_t^1 \times \mathcal{F}_t^2\right]$ to denote the expectation under Q conditional on the available information up to time t, so that formula (3.1) can be rewritten as

$$P_t = KE_t^Q\left[\sum_{s=\lfloor t \rfloor+1}^{T} D(t,s)\left(R + i_s\Pi\left(Y_{s-1}, Z_{s-1}\right)\right) + D(t,T)\Pi\left(Y_T, Z_T\right)\right]. \qquad (3.2)$$

3.2 On the pricing measure

In this section we discuss how to determine a pricing measure Q for the pricing formula (3.2).

Naturally, we employ the well-established arbitrage pricing theory for asset pricing (see, e.g., Björk 2009) to price the financial risks. That is, we use a risk-neutral probability measure Q^2 for the space $(\Omega^2, \mathcal{F}^2)$ to price the financial risks contained in Z to be the conditional expectation under Q^2 of the stochastic present value given available information.

Next we define a pricing measure Q^1 for the space $(\Omega^1, \mathcal{F}^1)$ that can be used to price the catastrophic insurance risks.

A distorted measure for catastrophic insurance risk pricing

Note that typically the underlying catastrophic insurance risks in the CAT bond cannot be hedged by existing assets in the insurance market, and the risk-neutral pricing framework does not apply to the pricing of such risks. To reflect investors' demand for catastrophic insurance risk premia, we employ the ideas of Denneberg (1994) and Wang (1996, 2000, 2002, 2004) to introduce a distorted probability measure as the pricing measure.

Let $g : [0,1] \to [0,1]$, with $g(0) = 0$ and $g(1) = 1$, be a distortion function and assume that it is differentiable on $[0,1]$ with a non-negative derivative of arbitrary order,

$$g^{(k)}(q) \geq 0, \qquad q \in [0,1],\ k = 0, 1, \ldots. \tag{3.3}$$

The latter is often called the absolute monotonicity condition (see, e.g., Di Bernardino and Rullière 2013).

Using g as the distortion function, we define a distorted probability measure Q^1 on $(\Omega^1, \mathcal{F}^1)$ by distorting the finite-dimensional distributions of $\{Y_t, t \geq 0\}$; that is, let

$$Q^1(Y_{t_1} \leq x_1, Y_{t_2} \leq x_2, \ldots, Y_{t_n} \leq x_n) = g \circ P^1(Y_{t_1} \leq x_1, Y_{t_2} \leq x_2, \ldots, Y_{t_n} \leq x_n) \tag{3.4}$$

hold for every $n \in \mathbb{N}$, every $\mathbf{t} \in [0,T]^n$ with $0 \leq t_1 < t_2 < \cdots < t_n \leq T$, and every $\mathbf{x} \in \mathbb{R}^n$. Note that this indeed defines a proper distribution function for $(Y_{t_1}, Y_{t_2}, \ldots, Y_{t_n})$. To see this, consider the case with $n = 3$ as an example. Denoting for simplicity by G the distribution of $(Y_{t_1}, Y_{t_2}, Y_{t_3})$ under P^1, we have

$$\begin{aligned}
& dg \circ G(x_1, x_2, x_3) \\
= \; & g^{(3)}\left(G(x_1, x_2, x_3)\right) G(dx_1, x_2, x_3) G(x_1, dx_2, x_3) G(x_1, x_2, dx_3) \\
& + g^{(2)}\left(G(x_1, x_2, x_3)\right) G(dx_1, dx_2, x_3) G(x_1, x_2, dx_3) \\
& + g^{(2)}\left(G(x_1, x_2, x_3)\right) G(dx_1, x_2, dx_3) G(x_1, dx_2, x_3) \\
& + g^{(2)}\left(G(x_1, x_2, x_3)\right) G(x_1, dx_2, dx_3) G(dx_1, x_2, x_3) \\
& + g^{(1)}\left(G(x_1, x_2, x_3)\right) G(dx_1, dx_2, dx_3).
\end{aligned}$$

Thus, condition (3.3) guarantees the non-negativity of $dg \circ G(x_1, x_2, x_3)$, which therefore defines a proper three-dimensional distribution function. Finally, by Kolmogorov's extension theorem (see, e.g., Theorem 2.1.5 of Øksendal 2003), there is a probability measure Q^1 under which Y has finite-dimensional distributions satisfying (3.4) above. This probability measure Q^1 will be the pricing measure to be used for catastrophic insurance risks.

Two remarks follow. First, as shown in their Proposition 2.1, in order for $Q^1(Y_{t_1} \leq x_1, Y_{t_2} \leq x_2, \ldots, Y_{t_n} \leq x_n)$ in (3.4) to be an absolutely continuous distribution, Di Bernardino and Rullière (2013) propose the absolute monotonicity condition (3.3) on g and an additional assumption that $(Y_{t_1}, Y_{t_2}, \ldots, Y_{t_n})$ possesses an absolutely continuous distribution under P^1. We point out that this additional assumption is unnecessary for our purpose. Second and more importantly, the condition $g^{(2)}(q) \geq 0$ for $q \in [0,1]$ in (3.3) implies that $g(q) \leq q$ for $q \in [0,1]$, and thus, for every $0 \leq t \leq T$

and $x \in \mathbb{R}$,

$$Q^1 (Y_t > x) = 1 - g \circ P^1 (Y_t \le x) \ge 1 - P^1 (Y_t \le x) = P^1 (Y_t > x).$$

This means that Y_t becomes more heavy-tailed (hence, riskier) under the distorted probability measure Q^1 than under the original probability measure P^1.

Below are some examples of distortion function satisfying the absolute monotonicity condition (3.3), the verification of which is relegated to Section 6.

Example 3.1 *Let g be defined on $[0,1]$.*

(i) (polynomial distortion) $g(q) = M(q)/M(1)$, where $M(q)$ is a nondegenerate polynomial function taking the form of

$$M(q) = a_n q^n + a_{n-1} q^{n-1} + \cdots + a_1 q$$

for $n \in \mathbb{N}$, $a_n > 0$, $a_{n-1} \ge 0$, $\ldots$, and $a_1 \ge 0$;

(ii) (exponential distortion) $g(q) = (e^{\lambda q} - 1)/(e^{\lambda} - 1)$ for some $\lambda > 0$;

(iii) (the Wang transform) $g(q) = \Phi\left(\Phi^{-1}(q) - \kappa\right)$ for some $\kappa > 0$, where Φ is the standard normal distribution.

The Wang transform has been widely used in the insurance literature because of its mathematical tractability. The single parameter κ reflects the extent to which the distribution under P^1 needs to be distorted to be more skewed toward the right for the pricing purpose and thus can be understood as the market price of risk. It is usually estimated by calibrating the model to the price data from existing deals and then used to price new deals.

A product measure for CAT bond pricing

Per the discussions above, we have obtained a pricing measure Q^1 for the catastrophe insurance market and a pricing measure Q^2 for the financial market. The independence assumption we made between the two markets suggests that, to price products with payoffs linked to both catastrophic insurance and financial risks, we should use the product measure $Q^1 \times Q^2$ as the pricing measure. Substituting $Q = Q^1 \times Q^2$ into (3.2) yields our general pricing formula, for $t \in [0,T]$,

$$P_t = K E_t^{Q^1 \times Q^2} \left[\sum_{s=\lfloor t \rfloor + 1}^{T} D(t,s) \left(R + i_s \Pi\left(Y_{s-1}, Z_{s-1}\right)\right) + D(t,T) \Pi\left(Y_T, Z_T\right) \right], \tag{3.5}$$

where $D(t,s)$, R, and i_t are defined as before.

Some authors have argued that, since the catastrophic insurance risks have only a marginal influence on the overall economy and do not pose systematic risk, it is unnecessary to price these risks and the risk premium should be set to zero; see, for example, Lee and Yu (2002). This may not be reasonable considering the fact that on the insurance market the catastrophes do have substantial and possibly systematic influence (see, e.g., Gürtler et al. 2016) and, hence, should be priced accordingly.

Moreover, in the literature the pricing measure for catastrophic insurance risks is sometimes obtained by simply attaching a constant risk premium c to the risk-free interest rate used in the pricing formula so that the discount factor $D(t,s)$ is modified to

$$\tilde{D}(t,s) = \exp\left\{-\int_t^s (r_u + c)\, du\right\},$$

regardless of the actual physical distribution of the underlying catastrophic insurance risk; see, for example, Zimbidis et al. (2007) and Shao et al. (2015). Such a pricing scheme may be questionable too since the resulting risk premia for catastrophes at different degrees have become indistinguishable. Our idea of introducing a pricing measure Q^1 is to link it directly to the underlying catastrophic insurance risk Y. If the catastrophic insurance risk Y fades out, then the CAT bond should converge to a usual bond in the arbitrage-free financial market. In this case, our pricing formula (3.5) remains valid because the distribution of Y under Q^2 becomes degenerate.

Other closely related discussions of pricing CAT bonds and CAT derivatives can be found in Cox and Pedersen (2000), Cox et al. (2000), Lin and Cox (2008), Muermann (2008), Egami and Young (2008), Ma and Ma (2013), and Nowak and Romaniuk (2013), among others. In particular, Egami and Young (2008) follow a different approach to pricing CAT bonds in an incomplete market. They apply the concept of indifference pricing to obtain a bond price that makes the bond issuer indifferent, in terms of expected utilities, between selling and not selling for that price. See also Barrieu and Loubergé (2009) and Leobacher and Ngare (2016) for some recent studies following this line.

An important special case

Here we show a significant simplification of the pricing formula (3.5) for an important special case where $\Pi(y,z)$ is reduced to $\Pi(y)$, a univariate function of the insurance risk trigger only. Under the general pricing framework introduced above, we make the following assumptions:

- The CAT bond is triggered only by the insurance risk trigger Y and, hence, $\Pi : [0,\infty) \to [0,1]$ reduces to a univariate, nonincreasing, and right-continuous function with $\Pi(0) = 1$
- $\{Y_t, t \geq 0\}$ is a Markov process with respect to the filtration $\{\mathcal{F}_t^1, t \geq 0\}$
- The Wang transform $g(\cdot) = \Phi\left(\Phi^{-1}(\cdot) - \kappa\right)$ for some $\kappa > 0$ is used as the distortion function defining Q^1.

Then by factorizing each expectation $E_t^{Q^1\times Q^2}$ in (3.5) into $E_t^{Q^1} \times E_t^{Q^2}$, the price of the CAT bond at $t \in [0,T]$ is expanded (and actually simplified) to

$$P_t \quad = \quad KR \sum_{s=\lfloor t \rfloor+1}^{T} E_t^{Q^2}\left[D(t,s)\right]$$

$$
\begin{aligned}
&+K \sum_{s=\lfloor t\rfloor+1}^{T} E_t^{Q^1}\left[\Pi\left(Y_{s-1}\right)\right] E_t^{Q^2}\left[D(t,s) i_s\right] \\
&+K E_t^{Q^1}\left[\Pi\left(Y_T\right)\right] E_t^{Q^2}\left[D(t,T)\right]. \qquad (3.6)
\end{aligned}
$$

For the computation of each expectation $E_t^{Q^1}[\Pi(Y_s)]$, assume that $Y = \{Y_t, t \geq 0\}$ is a time-homogenous Markov process with respect to the filtration $\{\mathcal{F}_t^1, t \geq 0\}$ under Q^1, as is often true. For $s = \lfloor t\rfloor$, we have $E_t^{Q^1}[\Pi(Y_s)] = \Pi(Y_{\lfloor t\rfloor})$. For $s = \lfloor t\rfloor + 1, \ldots, T$, by the Markov property of Y we have

$$
\begin{aligned}
E_t^{Q^1}\left[\Pi(Y_s)\right] &= E^{Q^1}\left[\Pi(Y_s) \middle| Y_t = y\right] \\
&= \int_0^1 Q^1\left(\Pi(Y_s) > u \middle| Y_t = y\right) du \\
&= \int_0^1 Q^1\left(Y_s < \Pi^{\leftarrow}(u) \middle| Y_t = y\right) du \\
&= \int_0^1 \Phi\left(\Phi^{-1}\left(1 - p_{s-t}(u|y)\right) - \kappa\right) du, \qquad (3.7)
\end{aligned}
$$

where $\Pi^{\leftarrow}$ denotes the generalized inverse of Π, defined by

$$
\Pi^{\leftarrow}(u) = \inf\left\{y \in \mathbb{R} : \Pi(y) \leq u\right\}, \qquad u \in [0,1],
$$

and $p_{s-t}(u|y)$ denotes the conditional probability

$$
p_{s-t}(u|y) = P^1\left(Y_s \geq \Pi^{\leftarrow}(u) \middle| Y_t = y\right).
$$

In the third step of (3.7), we have applied the fact that $\Pi(y) > u$ if and only if $y < \Pi^{\leftarrow}(u)$, which can be easily verified by the right-continuity of Π; see also Proposition A.3(iv) of McNeil et al. (2015) for a similar result. Thus, we need to evaluate the conditional distribution of Y_s given Y_t under the physical probability measure P^1 for every $s = \lfloor t\rfloor + 1, \ldots, T$. This is where EVT comes into play, as demonstrated in the following section.

4 Applications of the Pricing Theory

In this section, we apply the established approach through relation (3.6) to price two concrete CAT bonds.

4.1 CAT bond I

We consider an earthquake CAT bond in which the payoff function $\Pi(\cdot)$ is structured to apply to the magnitudes of major earthquakes. Usually, earthquake CAT bonds are triggered by the maximum magnitude of earthquakes or the number of earthquakes with a high magnitude. In the former case, relying on the Fisher–Tippett–Gnedenko theorem, one may apply the block maxima method to approximate the distribution of the maximum magnitude. We present details of this method in Section 6.2; see also Zimbidis et al. (2007) for related discussions. Note that, however, the block maxima method rests on the knowledge of the maxima for all blocks. This may not be the case when, for example, only major earthquakes with magnitude over a certain level are recorded. In this case the POT method can be used as an alternative. Here we present an example motivated by the Acorn Re 2015-1 CAT bond[8] (see also Example 1.3 in Section 1.3), where the POT method becomes particularly useful.

Example 4.1 Consider a T-year CAT bond with face value 1, in which the payoff function Π is defined by

$$\Pi(y) = 1 - y, \qquad y \geq 0,$$

and the insurance risk trigger Y_t is modeled by

$$Y_t = \min\left\{0.25N_1(t) + 0.5N_2(t) + 0.75N_3(t) + N_4(t),\ 1\right\}, \qquad t \geq 0, \tag{4.1}$$

with $N_1(t)$, $N_2(t)$, $N_3(t)$, and $N_4(t)$ denoting the numbers of earthquakes by time t with magnitude between 8.2 and 8.5, between 8.5 and 8.7, between 8.7 and 8.9, and over 8.9, respectively. This means that every occurrence of an earthquake with magnitude between, for example, 8.2 and 8.5 will wipe off 25% of the principal. The other specifications of the bond are as given in Section 3.1.

Data and estimation

We use the earthquake catalog data of California[9] provided by the California Department of Conservation's California Geological Survey to estimate the distribution of the earthquake magnitude. The data list information about earthquakes that occurred between 1769 and 2000 in California with a magnitude of at least 4.0, including the date and time of the occurrences, the latitudes and longitudes of their locations, and their magnitudes. The ones that occurred within 100 kilometers of the state border and therefore could still cause damage to properties in California are also included. Although data are available for the year 1769 through 2000, only the data set after 1942 is complete. The full data set for the year 1769 through 2000 contains 5,493 records. Four records have a date of 0, which are for earthquakes that happened before 1840. We interpret the dates of 0 as records missing and simply replace them by the first dates of the corresponding months. Also, we have deleted seven records with a magnitude of 0.

There may be multiple records of earthquake within a day for different locations across California. Since we are estimating the distribution of daily earthquake magnitude in California as a whole region, we use only the maximum record within a day. This leaves 3,484 records in the data set.

[8]Details can be found at `http://www.artemis.bm/deal_directory/acorn-re-ltd-series-2015-1/`.
[9]Available at `http://www.consrv.ca.gov/CGS/rghm/quakes/Pages/index.aspx`.

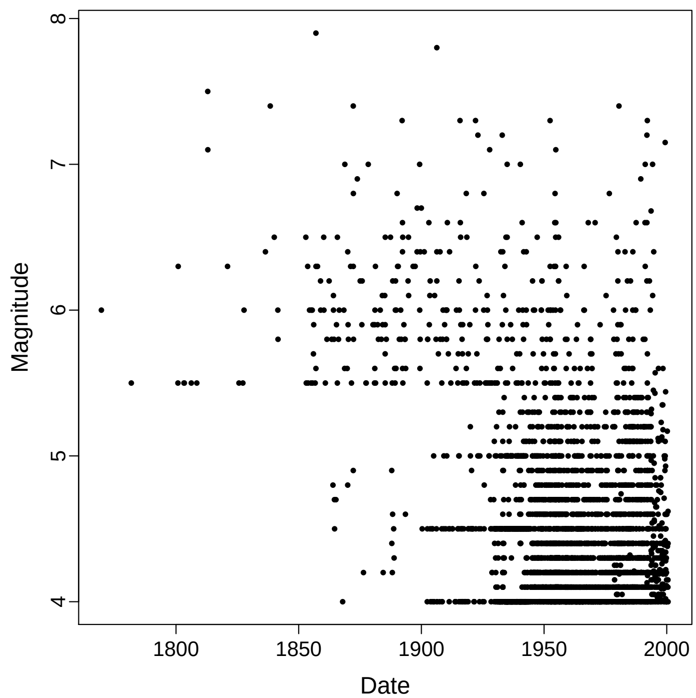

Figure 1. Scatter plot of earthquakes with magnitude 4.0 or greater.

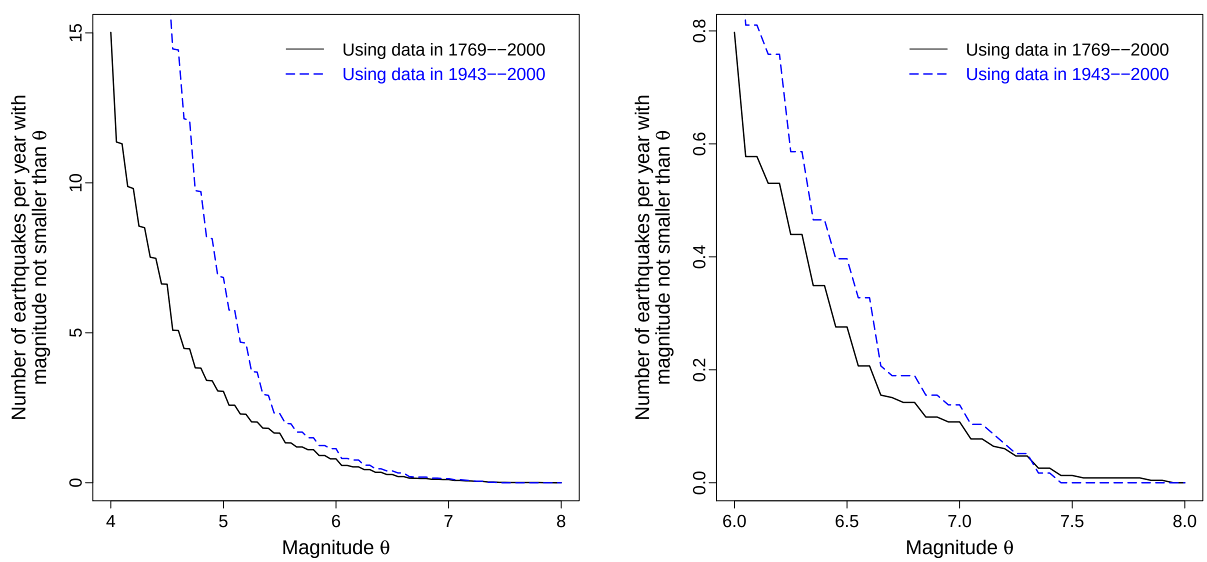

Figure 2. Frequency of earthquakes with magnitude θ or greater: a comparison between the full data (1769–2000) and the complete data (1943–2000).

From Figure 1 we see that there are significantly fewer records prior to the year 1942 than after, which is a clear indication of data missing. Nonetheless, we may reasonably assume that the major earthquakes prior to 1942 are still recorded in the data. We should take into consideration such large records because they will likely have a noticeable impact on the tail of the fitted earthquake magnitude distribution and, hence, are crucially important for our pricing purpose. To locate the part of data prior to 1942 that can be deemed complete, we show in Figure 2 a comparison between the full data (1769–2000) and the complete data (1943–2000) in terms of the frequency of earthquakes with a magnitude above some level.

The right graph of Figure 2 is a zoomed-in version of the left one for $\theta \geq 6.0$. Note the close frequencies of earthquakes starting from $\theta = 7.0$ for the two data sets. It is therefore reasonable to assume that in the full data the records of earthquakes of magnitude of 7.0 or greater are complete.

Using the complete data after 1942 we summarize our exploratory analysis in Figure 3.

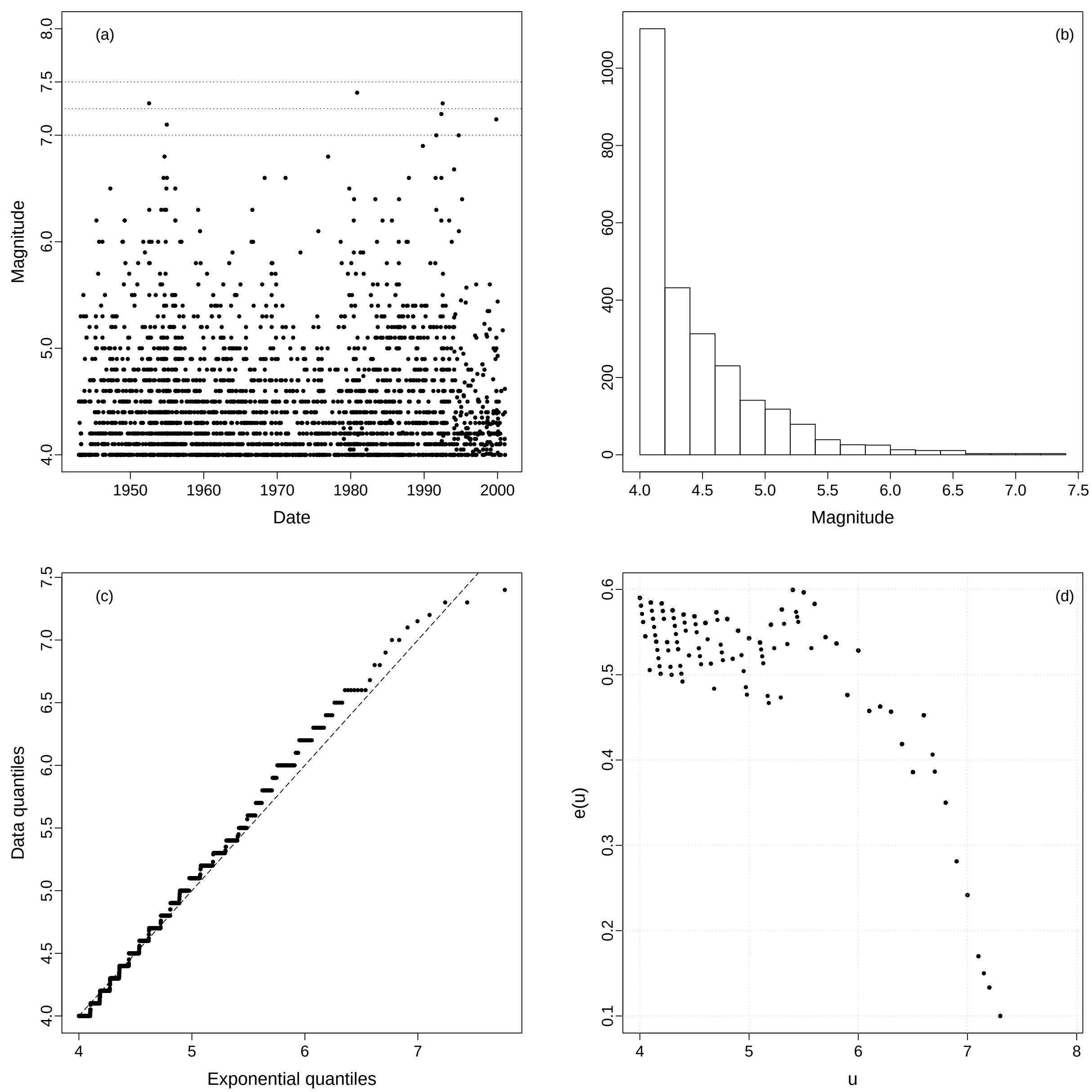

Figure 3. (a) Scatter plot. (b) Histogram. (c) QQ-plot. (d) Mean excess plot.

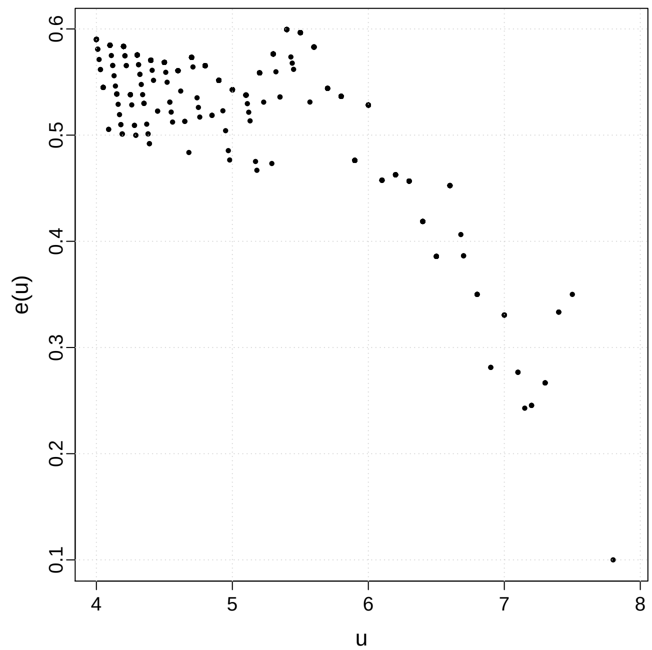

Figure 4. Mean excess plot with early records of earthquakes that have a magnitude of at least 7.

The graphs can offer us guidance to fit the earthquake magnitude distribution. To obtain a better fit in the tail area, we incorporate the large records prior to 1942 with magnitude 7.0 or greater and show a revised mean excess plot in Figure 4.

Recall from Section 2.2 that the mean excess plot of a GPD is linear. Therefore, Figure 3(d) suggests that we should be safe to consider using a GPD to fit the conditional distribution of the earthquake magnitude $\Theta|\Theta > y$. Although the choice of threshold is a trade-off between bias and variance and is indeed subjective, it is suggested that we use a graphical approach to choose a threshold y such that the empirical mean excess function is approximately linear beyond y. Therefore, a proper choice of the threshold can be $y = 5.0$; see Embrechts et al. (1999) for a similar discussion. In the complete data we find 334 records of 5.0 or greater, the exceedance probability $P(\Theta > y)$ is roughly estimated as $334/(365 \times 58) = 1.58\%$, and, hence, we may consider $y = 5.0$ as a high threshold.

We then implement an MLE procedure to estimate the GPD parameters ξ and β based on the full data set (1769–2000) of earthquakes with magnitude 7 or greater and the complete data set (1943–2000) of earthquakes with magnitude between 5.0 and 7.0. Specifically, let $\theta_1, \ldots, \theta_m$ be the observations of all earthquake magnitudes over 7.0, let $\theta_{m+1}, \ldots, \theta_{m+n}$ be those between 5.0 and 7.0, and let $\tilde{\theta}_j = \theta_j - 5$ be the exceedance over the threshold 5.0, $j = 1, \ldots, m+n$. In our data set, we have $m = 18$ and $n = 328$.

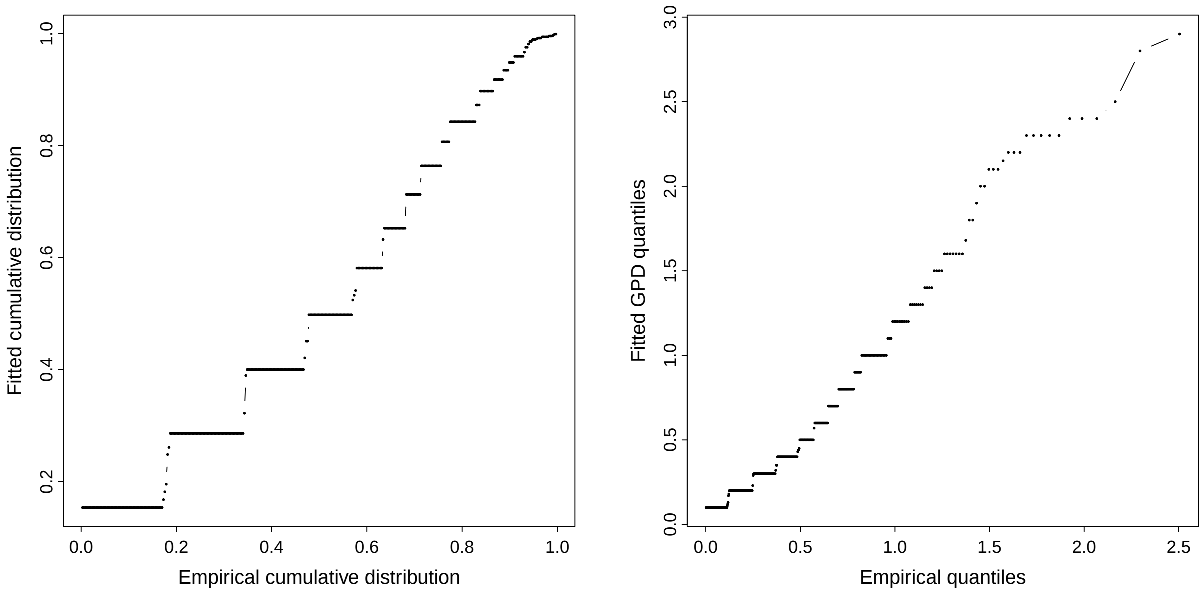

Figure 5. PP plot (left) and QQ plot (right) for model checking.

We use the R function `optim` to maximize the (conditional) log-likelihood function

$$l(\xi, \beta|\theta_1, \ldots, \theta_{m+n}) = \frac{m}{\xi} \ln(\beta + 2\xi) - n \ln\left(\beta^{-1/\xi} - (\beta + 2\xi)^{-1/\xi}\right) - \left(\frac{1}{\xi} + 1\right) \sum_{j=1}^{m+n} \ln\left(\beta + \xi\tilde{\theta}_j\right)$$

with respect to ξ and β, and we obtain $\hat{\xi} = -0.127$ and $\hat{\beta} = 0.606$. The MLEs are known to have good properties such as consistency and asymptotic efficiency for $\xi > -1/2$ (see Section 6.5 of Embrechts et al. 1997). The PP plot and QQ plot in Figure 5 show that the fitting is reasonably good. Nonetheless, we point out that the choice of the high threshold y may have a significant impact on the estimation results, as can be seen from the graph of mean excess function. A smaller value of y typically leads to estimates that correspond to a larger maximum possible magnitude of earthquake.

The bond price and sensitivity analysis

Our pricing framework involves a continuous-time risk-free interest rate process $\{r_t, t \geq 0\}$ and a discrete-time LIBOR process $\{i_t, t \in \mathbb{N}\}$, both defined on $(\Omega^2, \mathcal{F}^2)$. In order to apply some well-established continuous-time interest rate models, we consider a continuous-time version of the LIBOR process $\{\ell_t, t \geq 0\}$ and let $i_t = \ell_t$ for $t \in \mathbb{N}$ as an approximation. We model $\{r_t, t \geq 0\}$ and $\{\ell_t, t \geq 0\}$ as two correlated Cox–Ingersoll–Ross (CIR) processes (6.4) and (6.6), respectively, under the risk-neutral measure Q^2. We relegate precise model descriptions and related simulation algorithm to Section 6.3.

Further assume that daily earthquake magnitudes are i.i.d. random variables. Hence, the insurance risk trigger $\{Y_t, t \geq 0\}$ defined by (4.1) is a time-homogeneous Markov process. Then we may use relation (3.6) to price the bond.

Specifically, for each $s = \lfloor t \rfloor + 1, \ldots, T$, we shall simulate the value of $E_t^{Q^1}[\Pi(Y_s)]$ for a given value of Y_t, and simulate the value of

$$E_t^{Q^2}[D(t,s)\ell_s]$$

for given values of r_t and ℓ_t. The probability measure Q^1 is obtained through the Wang transform on the earthquake magnitude distribution directly with parameter κ, rather than on the trigger process $\{Y_t, t \geq 0\}$. Note that because the value of the trigger process is nondecreasing in the earthquake magnitudes, and because such a transform preserves all information needed for describing the trigger process, the measure Q^1 so obtained is sufficient for our pricing purpose.

Recall that at time 0 the pricing exercise is to find the fixed coupon rate R such that the bond price P_0 is equal to its face value 1. We now conduct numerical studies to demonstrate the impacts on the coupon rate of the Wang transform parameter κ, the risk-free interest rate, the maturity of the bond, and the parameters of the earthquake magnitude distribution.

In our base model, we assume that the CAT bond matures in one year. The base-model parameters of the two CIR models (6.4) and (6.6) are $a_r = 0.1$, $b_r = 3\%$, $\sigma_r = 0.03$, $r_0 = 1\%$, $a_\ell = 0.1$, $b_\ell = 3.5\%$, $\sigma_\ell = 0.04$, $\ell_0 = 1.5\%$, and $\rho = 0.9$. Under the probability measure P^1, the daily earthquake magnitudes are i.i.d. with a 1.58% probability of exceeding 5.0, and conditional on its exceedance the amount of exceedance follows a GPD with shape parameter $\xi = -0.127$ and scale parameter $\beta = 0.606$. To obtain the distorted measure Q^1 for pricing, we use the Wang transform with $\kappa = 1$.

Each expectation $E_t^{Q^1}[\Pi(Y_s)]$ is estimated using a simulation of 10^5 samples of the earthquake magnitude, simulated under Q^1, for each of the 360 days every year. In our sensitivity analysis, we always link the parameters ξ and β so that $\beta/\xi = -0.606/0.127$ and, hence, the upper endpoint of the earthquake magnitude distribution is fixed. We demonstrate the numerical results in Figures 6–11.

We observe the following:

- The Wang transform parameter κ as an indicator of the earthquake risk premium has a large impact on the CAT bond price (see Figure 6). A larger value of κ means a higher risk premium required by the bond investor and therefore a lower bond price. For example, an increase of κ from 0.8 to 1.5 increases the fixed coupon rate substantially from 0.41% to 13.38%. Note that a low market price of risk leads to negative fixed coupon rate, because in our setting it is guaranteed that the collateral will earn the floating coupon rate linked to LIBOR, with zero default probability, and hence when the demanded risk premium is low, the initial bond price cannot be below its face value.

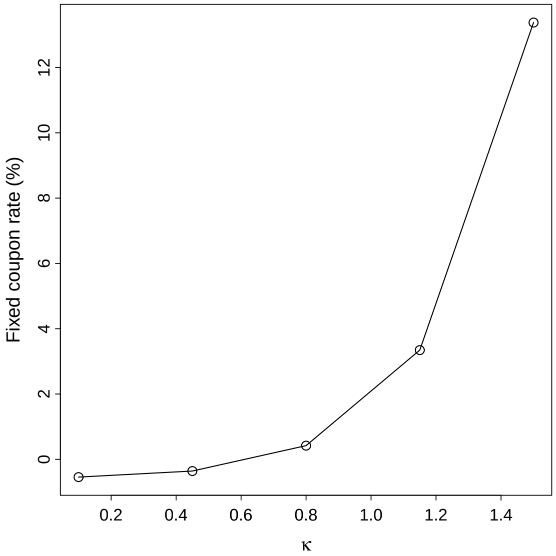

Figure 6. Change of the fixed coupon rate R with respect to κ.

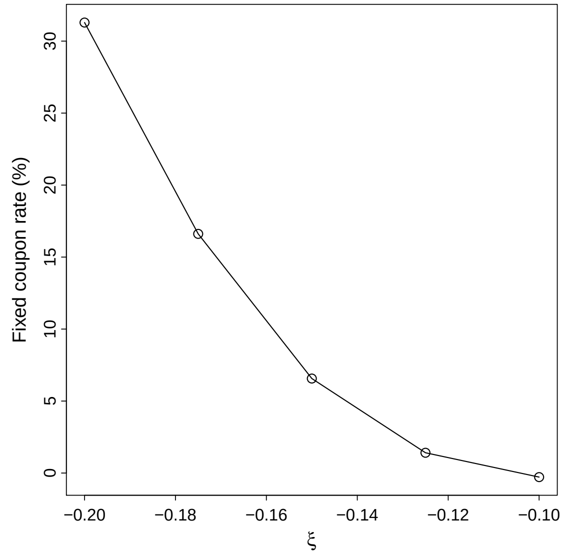

Figure 7. Change of the fixed coupon rate R with respect to ξ.

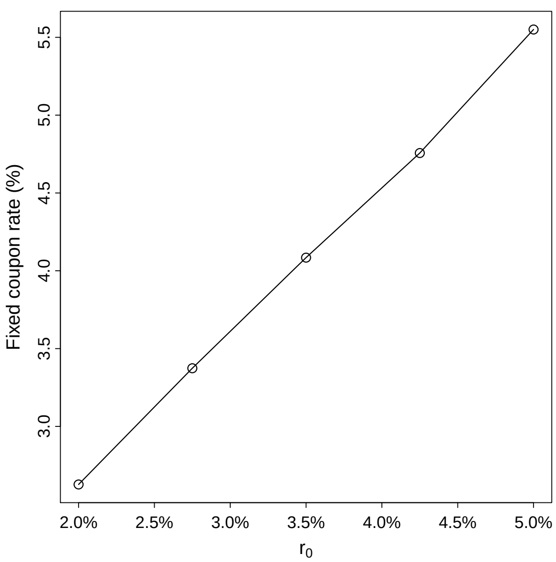

Figure 8. Change of the fixed coupon rate R with respect to r_0.

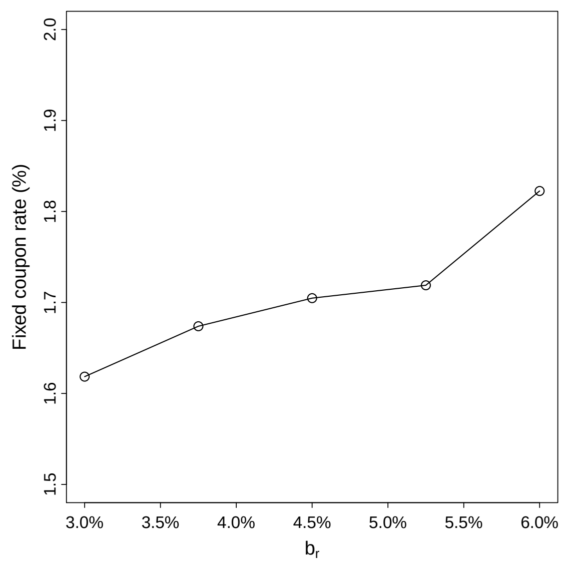

Figure 9. Change of the fixed coupon rate R with respect to b_r.

- The shape parameter ξ, which controls the tail behavior of the earthquake magnitude distribution, also has a great impact (see Figure 7). A smaller value of ξ (together with β adjusted according to $\beta/\xi = -0.606/0.127$) means a higher probability assigned to the tail and, hence, leads to a lower bond price. A decrease of ξ from -0.15 to -0.2 increases the fixed coupon rate dramatically from 6.57% to 31.29%.

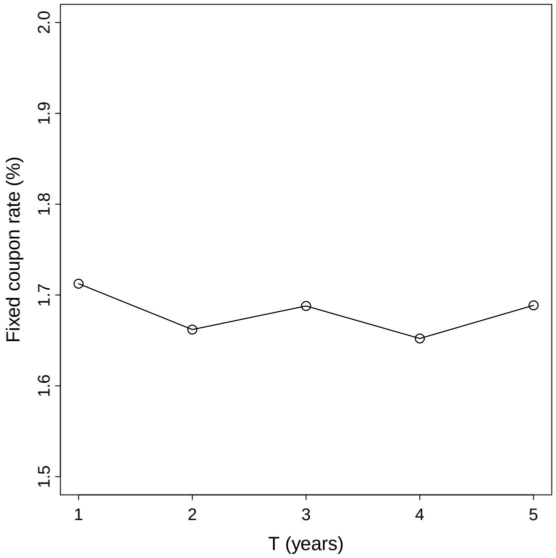

Figure 10. Change of the fixed coupon rate R with respect to T.

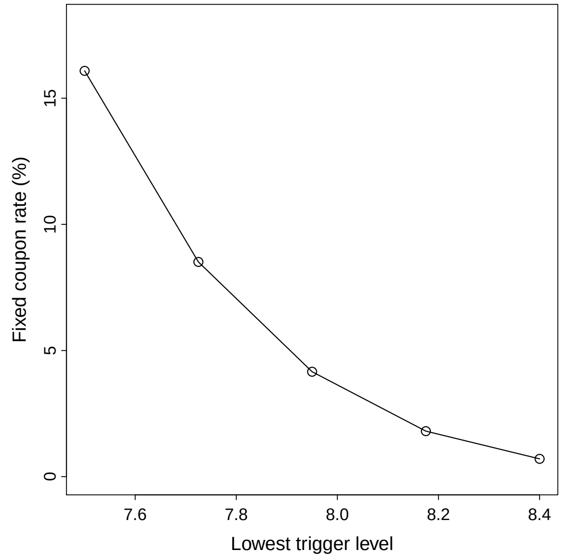

Figure 11. Change of the fixed coupon rate R with respect to the lowest trigger level.

- The current interest rate r_0 has a linear positive effect on R (see Figure 8), as is also clear from relations (3.6) and (6.5).
- As the long-term interest rate b_r increases, the fixed coupon rate also increases, although not substantially (see Figure 9).
- The bond maturity date does not affect the fixed coupon rate (see Figure 10), just as it does not for regular noncatastrophe bonds sold at par.
- Finally, it is anticipated that the trigger levels have an impact on the bond price. Figure 11 shows that changing only the lowest level of the trigger with the other three unchanged already leads to a significant change in the bond price.

Figure 12 shows a sample path of bond price evolution for a three-year bond, given a sample path of r_t and ℓ_t, assuming that a major earthquake with magnitude between 8.2 and 8.5 happens 10 months after the bond's issuance.

4.2 CAT bond II

In Section 4.1, the earthquake CAT bond we considered has the earthquake magnitude as a parametric trigger, while in this section we consider a CAT bond whose trigger depends on the aggregate loss of the sponsor or that of the entire industry. This applies to both indemnity-based and index-based triggers.

We specify the insurance risk trigger $\{Y_t, t \geq 0\}$ to be the aggregate loss process from a certain kind of catastrophes in d different regions. Suppose that the arrival of catastrophes in the d regions

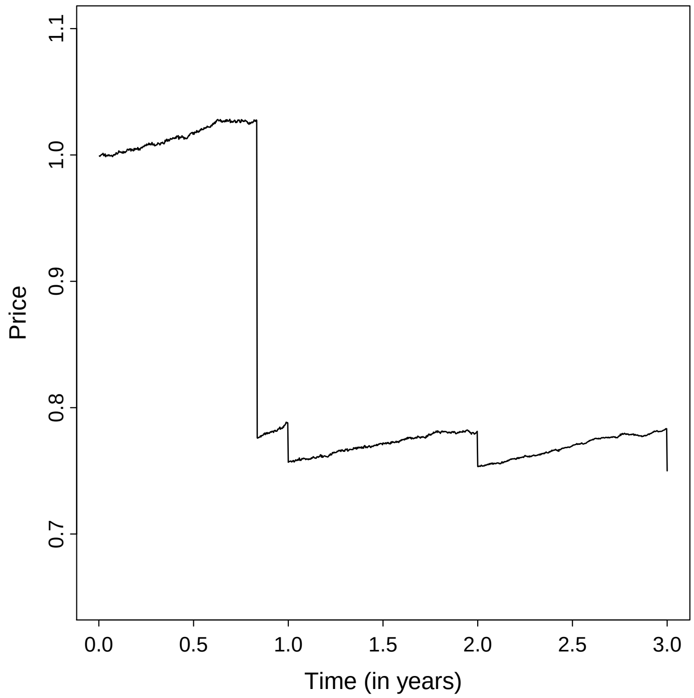

Figure 12. A sample path of bond price evolution.

share the same Poisson process N_t with intensity λ; that is, the number of catastrophes by time t is N_t. Suppose that the kth catastrophe in the jth region incurs a loss of amount $X_{jk} \geq 0$, and, hence, the total loss from the catastrophes in the jth region until time t is $\sum_{k=1}^{N_t} X_{jk}$. In this way, the aggregate loss over the d regions up to time t is given by

$$Y_t = \sum_{j=1}^{d} \sum_{k=1}^{N_t} X_{jk} = \sum_{k=1}^{N_t} \left(\sum_{j=1}^{d} X_{jk} \right), \tag{4.2}$$

which is a compound Poisson process (hence, a time-homogeneous Markov process) under P^1, assuming that $(X_{1k}, \ldots, X_{dk})$, $k = 1, 2, \ldots$, form a sequence of i.i.d. random vectors, independent of $\{N_t, t \geq 0\}$.

As before, we use a nonincreasing and right-continuous payoff function $\Pi : [0, \infty) \to [0, 1]$ with $\Pi(0) = 1$ to describe the reduction of the remaining principal according to the development of the aggregate loss process $\{Y_t, t \geq 0\}$. Furthermore, we introduce a reference loss variable Y, which is non-negative and distributed by G under P^1, and introduce a nonincreasing and right-continuous link function $\eta : [0, 1] \to [0, 1]$ with $\eta(0) = 1$ and $0 \leq \eta(1) < 1$. Then we define

$$\Pi(y) = \eta\left(G(y)\right), \tag{4.3}$$

meaning that the amount the principal will be wiped out by an aggregate loss of y depends on how the aggregate loss is compared to the reference variable Y.

In the payoff function Π defined above, η is a general link function and G is a general distribution function. In order to address extreme risks, specify the link function η as

$$\eta(q) = \begin{cases} 1, & q < q_1, \\ c, & q_1 \leq q < q_2, \\ 0, & q_2 \leq q, \end{cases} \tag{4.4}$$

for some $0 < q_1 < q_2 < 1$ and $0 < c < 1$. Thus, if $Y_t \geq G^{\leftarrow}(q_1)$, then the bond is triggered and the principal decreases to $100c\%$ of the original principal; if further $Y_t \geq G^{\leftarrow}(q_2)$, then the remaining principal vanishes. The reference variable Y is typically chosen to be comparable to Y_T in tail. For simplicity, we specify Y to be Y_T and correspondingly G to be F_T, the distribution function of Y_T. Then the payoff function $\Pi(y)$ defined by (4.3) becomes

$$\Pi(y) = \eta\left(F_T(y)\right). \tag{4.5}$$

In summary, the CAT bond we deal with in this section possesses the following structure:

Example 4.2 Consider a T-year CAT bond with face value 1. The insurance risk trigger $\{Y_t, t \geq 0\}$ is specified to be the aggregate loss process from a certain kind of catastrophes in d different regions and modeled by the compound Poisson process (4.2). The payoff function Π is defined by (4.5) with η given by (4.4). The other specifications of the bond are as given in Section 3.1.

The tail probability of the aggregate losses under an MRV structure

Recall the aggregate loss process (4.2) in which $(X_{1k}, \ldots, X_{dk})$, $k = 1, 2, \ldots$, form a sequence of i.i.d. random vectors with generic vector $\mathbf{X} = (X_1, \ldots, X_d)$. Assume that $\mathbf{X} \in \mathrm{MRV}_{-\alpha}$; that is, relation (2.4) holds for some distribution function F with tail $\overline{F} \in \mathrm{RV}_{-\alpha}$ and some nonzero limit measure ν. As mentioned before, the tail dependence of $\mathbf{X}$ is reflected by the limit measure ν and can span from asymptotic independence to asymptotic dependence. Applying relation (2.6), we have, as $x \to \infty$,

$$P^1\left(\sum_{j=1}^{d} X_j > x\right) \sim \nu(A)\overline{F}(x),$$

where $A = \left\{\mathbf{z} \in [\mathbf{0}, \boldsymbol{\infty}] : \sum_{j=1}^{d} z_j > 1\right\}$. Here and throughout the report, the notation $\sim$ means that the ratio of both sides tends to 1. Moreover, we have

$$\begin{aligned} P^1\left(Y_t > x\right) &= P^1\left(\sum_{k=1}^{N_t}\sum_{j=1}^{d} X_{jk} > x\right) \\ &\sim \lambda t P^1\left(\sum_{j=1}^{d} X_j > x\right) \\ &\sim \lambda t \nu(A)\overline{F}(x), \end{aligned} \tag{4.6}$$

where the second step can be obtained by applying the dominated convergence theorem and the well-established subexponentiality theory; see Theorem 1.3.9 of Embrechts et al. (1997). One may introduce a microstructure for the loss vector $\mathbf{X}$ to refine the value of $\nu(A)$.

On the bond price

To obtain the bond price, first we still apply relation (3.7) to compute the expectations $E_t^{Q^1}\left[\Pi\left(Y_s\right)\right]$, $s>t$. Note that, as $q_1 \uparrow 1$, it holds uniformly for $0 \leq u < 1$ that $\Pi^{\leftarrow}(u) \geq F_T^{\leftarrow}(q_1) \uparrow \infty$. Therefore, for every $s \in (t, T]$, it follows from (4.6) that, uniformly for $0 \leq u < 1$,

$$
\begin{aligned}
p_{s-t}(u|y) &= P^1\left(Y_s \geq \Pi^{\leftarrow}(u) \middle| Y_t = y\right) \\
&= P^1\left(\sum_{k=1}^{N_{s-t}} \sum_{j=1}^{d} X_{jk} \geq \Pi^{\leftarrow}(u) - y\right) \\
&\sim \lambda(s-t)\nu(A)\overline{F}(\Pi^{\leftarrow}(u) - y).
\end{aligned}
$$

Then Lemma 6.1 allows us to further approximate $E_t^{Q^1}\left[\Pi(Y_s)\right]$ in (3.7) by

$$
1 - \int_0^1 \overline{\Phi}\left(\Phi^{-1}\left(1 - \lambda(s-t)\nu(A)\overline{F}(\Pi^{\leftarrow}(u) - y)\right) - \kappa\right) du.
$$

This may be useful when the quantity $\nu(A)\overline{F}(\Pi^{\leftarrow}(u) - y)$ is easily computable. In fact, in this simple example, it is easy to verify that the quantity above can be further expressed as follows:

Proposition 4.1 *As $q_1 \uparrow 1$, it holds for every $s \in (t, T]$ that*

$$
\begin{aligned}
& E^{Q^1}\left[\Pi(Y_s) \middle| Y_t = y\right] \\
= \; & 1 - (1+o(1))(1-c)\overline{\Phi}\left(\Phi^{\leftarrow}\left(1 - \lambda(s-t)\nu(A)\overline{F}\left(F^{\leftarrow}\left(1 - \frac{1-q_1}{\lambda T \nu(A)}\right) - y\right)\right) - \kappa\right) \\
& -(1+o(1))c\overline{\Phi}\left(\Phi^{\leftarrow}\left(1 - \lambda(s-t)\nu(A)\overline{F}\left(F^{\leftarrow}\left(1 - \frac{1-q_2}{\lambda T \nu(A)}\right) - y\right)\right) - \kappa\right), \qquad (4.7)
\end{aligned}
$$

where $A = \left\{\mathbf{z} \in [\mathbf{0}, \boldsymbol{\infty}] : \sum_{j=1}^{d} z_j > 1\right\}$.

We still assume that, under the risk-neutral measure Q^2, the risk-free interest rate $\{r_t, t \geq 0\}$ and the LIBOR rate $\{\ell_t, t \geq 0\}$ follow two correlated CIR processes given by (6.4) and (6.6), respectively. Then substituting the right-hand side of (4.7) into our general pricing formula (3.6) and using the algorithm described in Section 6.3 to simulate $E_t^{Q^2}\left[D(t,s)i_s\right]$, $s = \lfloor t \rfloor + 1, \ldots, T$, we obtain an approximation for the bond price.

Sensitivity analysis

We now conduct numerical studies to demonstrate the relationship between the fixed coupon rate, calculated using the approximation in relation (4.7), and various other parameters. In our base model, we consider a one-year CAT bond that covers $d = 5$ regions. The base-model parameters of the two CIR models are the same as in Section 4.1; that is, we set $a_r = 0.1$, $b_r = 3\%$, $\sigma_r = 0.03$, $r_0 = 2\%$, $a_\ell = 0.1$, $b_\ell = 3.5\%$, $\sigma_\ell = 0.04$, $\ell_0 = 2.5\%$, and $\rho = 0.9$. The base-model parameters in the payoff function Π are chosen to be $c = 0.5$, $q_1 = 98\%$, and $q_2 = 99.9\%$.

Moreover, the jump intensity λ is set to 1. The random vector $\mathbf{X} = (X_1, \ldots, X_d)$ is assumed to have Pareto marginal distributions with shape parameter 2 and scale parameter 1 and possess a Gumbel copula with parameter 2. This is known to yield an MRV structure for $\mathbf{X}$; see, for example, Lemma 5.2 of Tang and Yuan (2013). To obtain the distorted measure Q^1, we use the Wang transform with $\kappa = 0.5$ in the base model.

The numerical results are summarized in Figures 13–18. As before, we notice that the Wang transform parameter κ has a great impact on the CAT bond price (see Figure 13). An increase of κ from 0.8 to 1.5 would increase the fixed coupon rate substantially from 5.2% to 16.7%. The current interest rate r_0 still has a positive linear effect on the fixed coupon rate (see Figure 14), and the long-term interest rate b_r still has a modest effect on the fixed coupon rate (see Figure 15). Unlike the previous case, an increase of the maturity increases the aggregate loss at maturity and, hence, the quantile trigger level, and as a result, the fixed coupon rate is decreased (see Figure 16). Finally, a decrease of c or q_1 decreases the remaining principal and, hence, increases the fixed coupon rate (see Figures 17–18).

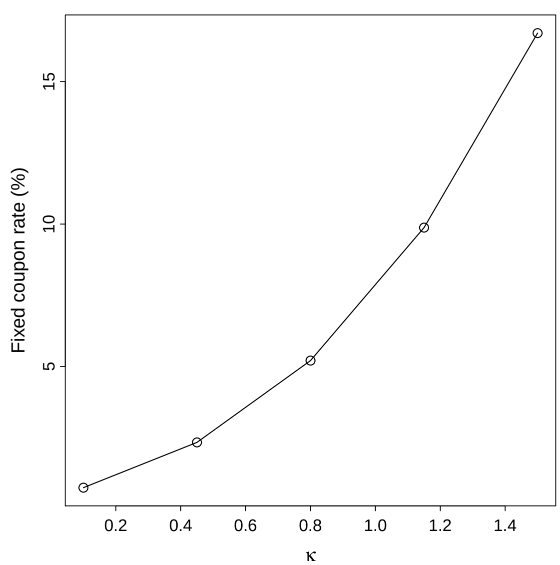

Figure 13. Change of the fixed coupon rate R with respect to κ.

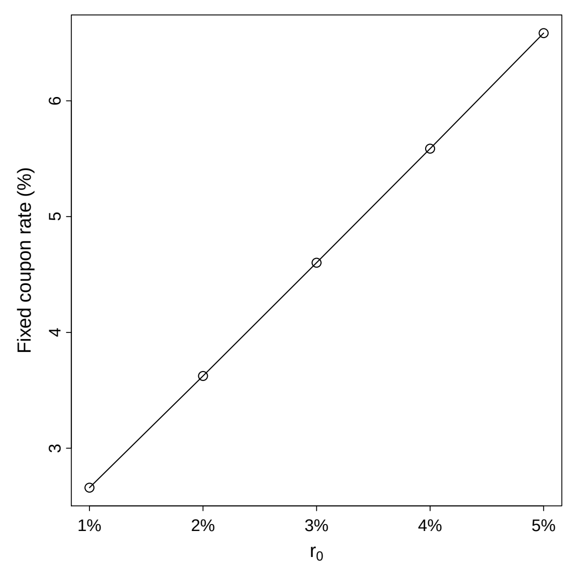

Figure 14. Change of the fixed coupon rate R with respect to r_0.

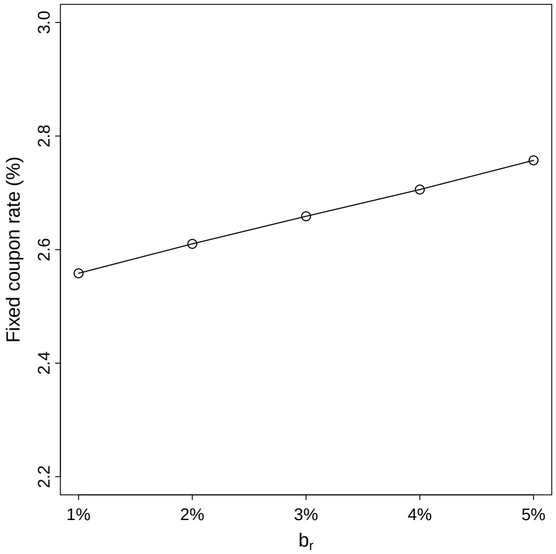

Figure 15. Change of the fixed coupon rate R with respect to b_r.

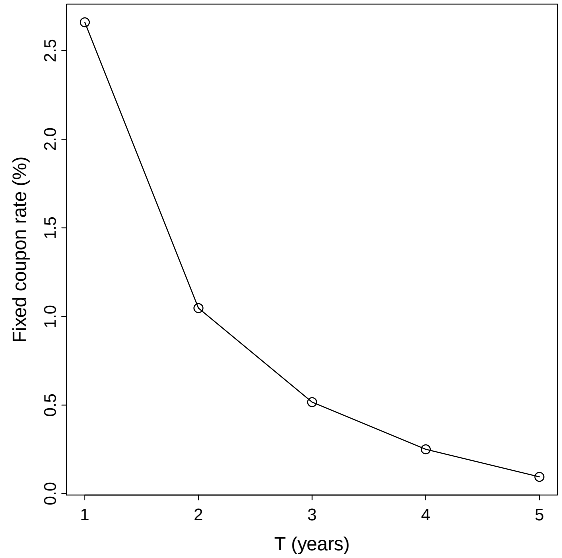

Figure 16. Change of the fixed coupon rate R with respect to T.

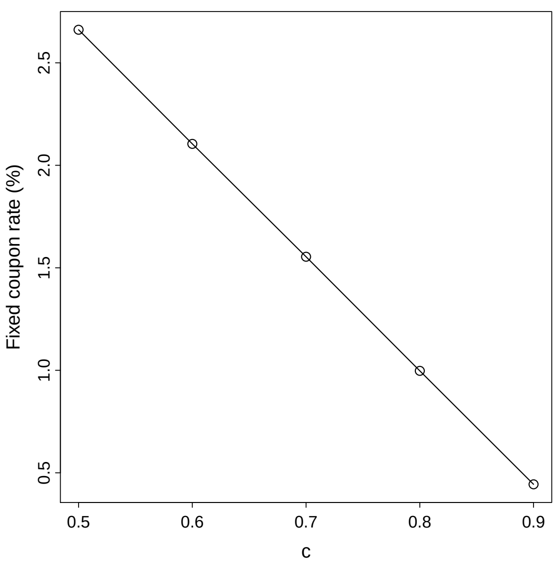

Figure 17. Change of the fixed coupon rate R with respect to c.

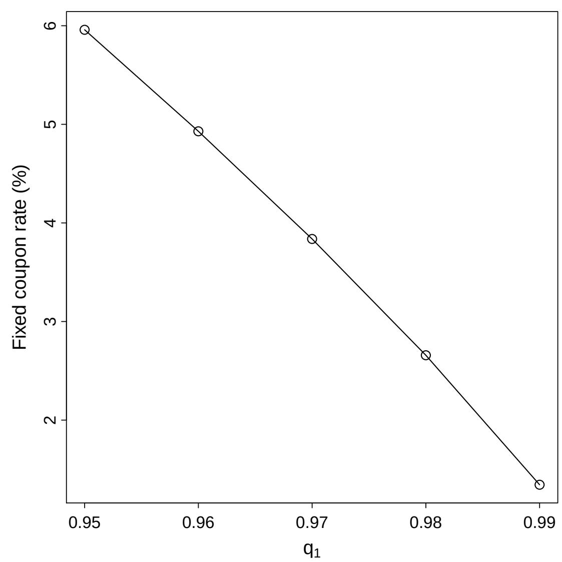

Figure 18. Change of the fixed coupon rate R with respect to q_1.

5 Quantifying the Basis Risk of ILWs

A well-known problem related to the use of an index-linked catastrophic loss instrument in the context of hedging is basis risk. This arises when, for example, the dependence between the company's loss and the industry loss is not sufficiently strong, and, hence, the former is not a good representative of the latter. In this section we shall discuss quantification of the basis risk in the use of dual-triggered ILWs, as well as the sensitivity of the basis risk to the dependence between the company's loss and the industry loss.

Consider a dual-triggered ILW that reimburses the purchaser/insurer if both its own loss and the industry-wide loss are above certain levels. Specifically, the ILW is assumed to have the payoff

$$\Pi^{\text{ILW}} = \left((X - x)_+ \wedge l\right) 1_{(Y>y)}, \tag{5.1}$$

where X and Y are two non-negative random variables representing the insurer's loss due to prescribed catastrophic events and the value of an industry loss index, respectively, l is the coverage limit, and x and y are the company- and industry-level attachment points, respectively. Similar ILW payoffs have appeared in, for instance, Cummins et al. (2004) and Gatzert and Kellner (2011). We discuss the cases with the company-level attachment point being average sized and being large, and we use different models to feature the two cases.

5.1 Average-sized attachment points

For the case with average-sized attachment points, following Zeng (2000) and Ross and Williams (2009), we quantify the basis risk of the ILW defined in (5.1) as the conditional probability that the insurer does not receive a payoff given that its loss X has surpassed the attachment point x; that is,

$$\text{BR} = P\left(Y \le y \middle| X > x\right). \tag{5.2}$$

We look at the microstructure of the losses that constitute X and Y, and we model the industry loss Y during a prescribed period using a compound Poisson structure

$$Y = \sum_{j=1}^{N(\lambda)} Z_j,$$

where $N(\lambda)$ is a Poisson random variable, with intensity $\lambda > 0$, counting the number of losses, and Z_j, $j = 1, 2, \ldots$, are sizes of individual losses, assumed to be i.i.d. non-negative random variables with common mean μ and variance σ^2 and independent of $N(\lambda)$. The number of losses this specific insurer will encounter is still a Poisson random variable, which we denote by $N_1(\theta_\lambda)$ with $0 \le \theta_\lambda \le \lambda$ representing its Poisson intensity. The number of the remaining losses is again a Poisson random variable, which we denote by $N_2(\lambda - \theta_\lambda)$ with intensity $\lambda - \theta_\lambda$. Within this Poisson framework, $N_1(\theta_\lambda)$ and $N_2(\lambda - \theta_\lambda)$ are two independent Poisson numbers, and, as a result, X and $Y - X$ are two independent random variables jointly identical in distribution to

$$(S_1, S_2) = \left(\sum_{j=1}^{N_1(\theta_\lambda)} Z_j, \sum_{j=N_1(\theta_\lambda)+1}^{N_1(\theta_\lambda)+N_2(\lambda-\theta_\lambda)} Z_j \right).$$

Assume that, as $\lambda \to \infty$,

$$\begin{cases} 0 \le \theta_\lambda \to \infty, \\ 0 \le \lambda - \theta_\lambda \to \infty, \\ \theta_\lambda/\lambda \to \theta \in [0, 1]. \end{cases}$$

The quantity θ in the last assumption above roughly represents this specific insurer's market share in the insurance market.

Choose the company-level attachment point x to be the $100p$th quantile of X, and choose the industry-level attachment point y to be the $100q$th quantile of Y for $p, q \in (0,1)$. By the central limit theorem (CLT), as $\lambda \to \infty$, the normalized quantities

$$\tilde{S}_1 = \frac{S_1 - \theta_\lambda \mu}{\sqrt{\theta_\lambda (\mu^2 + \sigma^2)}}, \qquad \tilde{S}_2 = \frac{S_2 - (\lambda - \theta_\lambda)\mu}{\sqrt{(\lambda - \theta_\lambda)(\mu^2 + \sigma^2)}}, \qquad \text{and} \qquad \tilde{Y} = \frac{Y - \lambda\mu}{\sqrt{\lambda (\mu^2 + \sigma^2)}}$$

all converge in distribution to $N(0,1)$. Thus, x and y, as the $100p$th and $100q$th quantiles of X and Y, respectively, satisfy

$$\begin{cases} x = \theta_\lambda \mu + \Phi^{-1}(p)\sqrt{\theta_\lambda (\mu^2 + \sigma^2)} + o(\sqrt{\lambda}), \\ y = \lambda\mu + \Phi^{-1}(q)\sqrt{\lambda (\mu^2 + \sigma^2)} + o(\sqrt{\lambda}). \end{cases}$$

We have

$$\begin{aligned} \mathrm{BR} &= P\left(S_1 + S_2 \le y \middle| S_1 > x\right) \\ &= \frac{P\left(S_1 + S_2 \le y, S_1 > x\right)}{P\left(S_1 > x\right)} \\ &= \frac{P\left(\sqrt{\frac{\theta_\lambda}{\lambda}}\tilde{S}_1 + \sqrt{\frac{\lambda - \theta_\lambda}{\lambda}}\tilde{S}_2 \le \Phi^{-1}(q) + o(1), \tilde{S}_1 > \Phi^{-1}(p) + o(1)\right)}{P\left(\tilde{S}_1 > \Phi^{-1}(p) + o(1)\right)}. \end{aligned}$$

Recall that $\tilde{S}_1$ and $\tilde{S}_2$ are independent and both converge in distribution to $N(0,1)$ as $\lambda \to \infty$. We conclude the following result, which represents a CLT solution to measuring the basis risk:

Theorem 5.1 *Consider the basis risk defined by (5.2). Under the assumptions above, it holds for every $p, q \in (0,1)$ that*

$$\lim_{\lambda \to \infty} \mathrm{BR} = \frac{1}{1-p} P\left(\sqrt{\theta}\eta_1 + \sqrt{1-\theta}\eta_2 \le \Phi^{-1}(q), \eta_1 > \Phi^{-1}(p)\right), \tag{5.3}$$

where η_1 and η_2 are two i.i.d. $N(0,1)$ random variables.

Two extreme cases are $\theta = 0$ and $\theta = 1$. The first case means that this insurer occupies a negligible market share of the whole industry, and the result above shows that the basis risk is approximately $1 - q$, while the second case means that this insurer's business dominates the whole industry, and the result above shows that the basis risk is approximately $\frac{q-p}{1-p} \vee 0$.

We conduct a numerical study of how the basis risk, approximated by relation (5.3), is influenced by the parameters θ and q, and we show the results in Figures 19–20. We observe that the basis risk decreases in θ, the market share of the insurer, and that it increases in q, the quantile level of the index trigger. Both observations are intuitively clear.

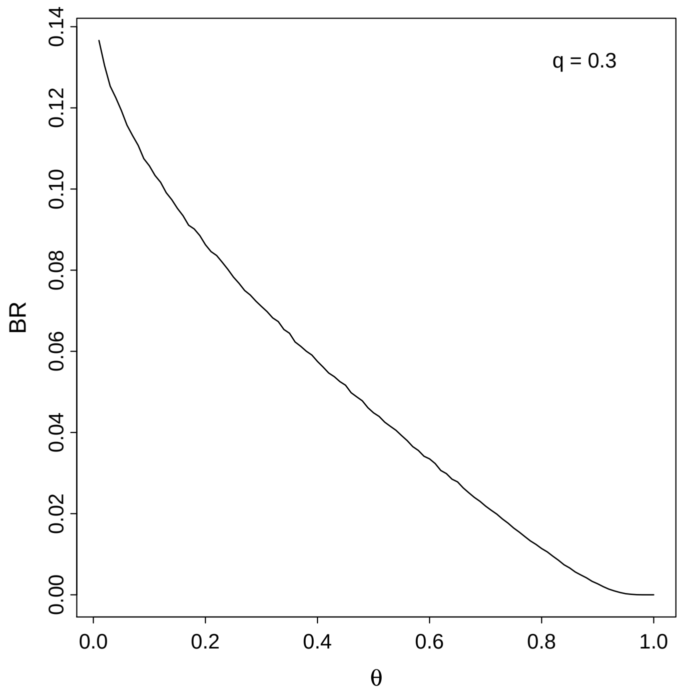

Figure 19. Change of the basis risk with respect to θ.

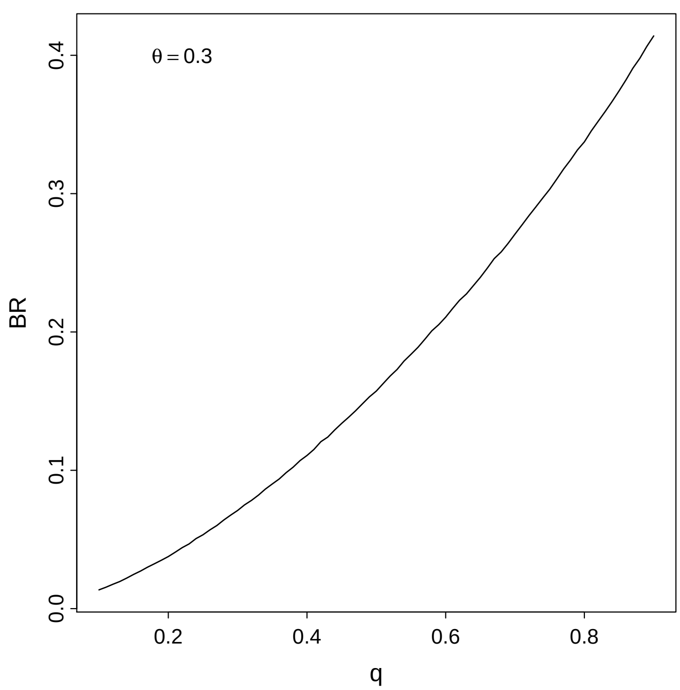

Figure 20. Change of the basis risk with respect to q.

5.2 Large attachment points

In this section, we consider the case where the company level attachment point x is large. To quantify the basis risk of the ILW with payoff given by (5.1), we now follow Gatzert and Kellner (2011) to use a traditional reinsurance contract and a hypothetical "perfect" ILW contract as benchmarks for perfect hedging. The traditional reinsurance contract has a payoff of

$$\Pi^{\mathrm{re}} = (X - x)_+ \wedge l. \tag{5.4}$$

In the "perfect" ILW the industry risk profile perfectly matches that of the insurer, and it has a payoff of

$$\Pi^{\mathrm{pe}} = \left((X - x)_+ \wedge l\right) 1_{(Y^c > y)}, \tag{5.5}$$

where Y^c is identical in distribution to Y and comonotonic with X. One sees that the traditional reinsurance corresponds to a special case of the ILW defined in (5.1) with $y = 0-$, and the "perfect" ILW corresponds to another special case of the ILW with the company loss X and the industry loss index Y being comonotonic. The hedged losses become

$$\begin{cases} L^{\mathrm{ILW}} = X - \left((X - x)_+ \wedge l\right) 1_{(Y > y)}, \\ L^{\mathrm{re}} = X - (X - x)_+ \wedge l, \\ L^{\mathrm{pe}} = X - \left((X - x)_+ \wedge l\right) 1_{(Y^c > y)}, \end{cases}$$

while being hedged by the ILW in (5.1), the traditional reinsurance in (5.4), and the "perfect" ILW in (5.5), respectively. According to Gatzert and Kellner (2011), we quantify the hedge effectiveness of each product as the counter-value of the proportional reduction in the VaR of the loss,

$$\mathrm{HE}^* = 1 - \frac{\mathrm{VaR}_q\left[L^*\right]}{\mathrm{VaR}_q\left[X\right]}, \qquad 0 < q < 1, \tag{5.6}$$

where $*$ stands for ILW, re, or pe, and then we quantify the basis risk of the ILW as the counter-value of the proportional reduction in hedge effectiveness,

$$\mathrm{BR}^{\mathrm{re}} = 1 - \frac{\mathrm{HE}^{\mathrm{ILW}}}{\mathrm{HE}^{\mathrm{re}}}, \qquad \mathrm{BR}^{\mathrm{pe}} = 1 - \frac{\mathrm{HE}^{\mathrm{ILW}}}{\mathrm{HE}^{\mathrm{pe}}}. \tag{5.7}$$

It is easy to see that $\mathrm{BR}^{\mathrm{re}} \geq 0$. This is because $L^{\mathrm{ILW}} \geq L^{\mathrm{re}}$ almost surely, which implies that $\mathrm{VaR}_q\left[L^{\mathrm{ILW}}\right] \geq \mathrm{VaR}_q\left[L^{\mathrm{re}}\right]$, and, hence, that $\mathrm{HE}^{\mathrm{re}} \geq \mathrm{HE}^{\mathrm{ILW}}$. However, the non-negativity of $\mathrm{BR}^{\mathrm{pe}}$ is not guaranteed, since we cannot assert a stochastic dominance between L^{ILW} and L^{pe}.

We are interested in the situation with a large company-level attachment point x, meaning that the ILW is designed to hedge extreme risks, and a high level q for the VaR, meaning to measure extreme risks. In such a situation, the CLT is no longer useful, and we instead employ an EVT approach to find asymptotic estimations for $\mathrm{BR}^{\mathrm{re}}$ and $\mathrm{BR}^{\mathrm{pe}}$ defined in (5.7).

To this end, assume that the company loss X and the industry loss index Y are distributed by F and G, respectively, with $\overline{F} \in \mathrm{RV}_{-\alpha}$ for some $\alpha > 0$. Furthermore, they possess a copula C

whose survival copula $\hat{C}$, defined to be

$$\hat{C}(u,v) = u + v - 1 + C(1-u, 1-v), \qquad (u,v) \in (0,1)^2,$$

satisfies

$$\lim_{s\downarrow 0} \frac{\hat{C}(su, sv)}{s} = H(u,v), \qquad (u,v) \in [0,\infty)^2 \tag{5.8}$$

for some bivariate, nondegenerate, and continuous function H on $[0,\infty)^2$. The function H describes the tail dependence structure of (X,Y) and is usually called a tail dependence function; see Jaworski (2004) and Joe et al. (2010). Clearly, $H(u,0) = H(0,v) = 0$, $H(u,\infty) = u$, and $H(\infty,v) = v$ for $(u,v) \in [0,\infty)^2$. Thus, with the convention that $H(\infty,\infty) = \infty$, relation (5.8) holds for $(u,v) \in [0,\infty]^2$. Furthermore, H is 2-increasing; that is, the inequality

$$H(u_2,v_2) - H(u_1,v_2) - H(u_2,v_1) + H(u_1,v_1) \geq 0$$

holds for every $0 \leq u_1 \leq u_2 \leq \infty$ and $0 \leq v_1 \leq v_2 \leq \infty$, because $\hat{C}$ as a copula is 2-increasing. We remark that the degree of dependence between X and Y described by (5.8) spans the dependence level from asymptotic independence to asymptotic dependence. In particular, if X and Y are comonotonic, as is the case for the "perfect" ILW, the function H reduces to $u \wedge v$.

Moreover, assume that the coverage limit l, the industry-level attachment point y, and the VaR level q are associated with the company-level attachment point x according to

$$\lim_{x\uparrow\infty} \frac{l}{x} = c_l, \qquad \lim_{x\uparrow\infty} \frac{\overline{G}(y)}{\overline{F}(x)} = c_y, \qquad \text{and} \qquad \lim_{x\uparrow\infty} \frac{1-q}{\overline{F}(x)} = b \tag{5.9}$$

for some $1 \leq c_l \leq \infty$, $0 \leq c_y \leq \infty$, and $0 < b \leq \infty$. Note that in the case of the traditional reinsurance, we have $y = 0-$ and consequently $c_y = \infty$.

For a nonincreasing function h, as in Section 3.2, its general inverse is defined by

$$h^{\leftarrow}(x) = \inf\{y \in \mathbb{R} : h(y) \leq x\}.$$

The following lemma provides an asymptotic approximation for the VaR of the hedged loss,

Lemma 5.1 *Under the assumptions above, as $x \uparrow \infty$, we have*

$$\mathrm{VaR}_q[L^{\mathrm{ILW}}] \sim \begin{cases} h^{\leftarrow}(b)x, & \text{for } 0 < b \leq h(1), \\ x, & \text{for } h(1) < b \leq 1, \\ b^{-1/\alpha}x, & \text{for } b > 1, \end{cases} \tag{5.10}$$

where

$$h(u) = u^{-\alpha} + H\left((c_l+u)^{-\alpha}, c_y\right) - H\left(u^{-\alpha}, c_y\right). \tag{5.11}$$

Note that $u^{-\alpha} - H\left(u^{-\alpha}, c_y\right) = H\left(u^{-\alpha}, \infty\right) - H\left(u^{-\alpha}, c_y\right)$ is nonincreasing in u by the 2-increase of H. Thus, h is a nonincreasing function, and the general inverse $h^{\leftarrow}$ is well defined.

As mentioned before, in the case of the traditional reinsurance, $c_y = \infty$, and consequently the function h is simplified to

$$h_1(u) = (c_l + u)^{-\alpha}.$$

It follows from Lemma 5.1 that

$$\mathrm{VaR}_q[L^{\mathrm{re}}] \sim \begin{cases} \left(b^{-1/\alpha} - c_l\right) x, & \text{for } 0 < b \leq (c_l+1)^{-\alpha}, \\ x, & \text{for } (c_l+1)^{-\alpha} < b \leq 1, \\ b^{-1/\alpha} x, & \text{for } b > 1. \end{cases} \tag{5.12}$$

Also as mentioned before, the "perfect" ILW is another special case of the ILW with the bivariate function $H(u, v)$ simplified to $u \wedge v$. Thus, it also follows from Lemma 5.1 that

$$\mathrm{VaR}_q[L^{\mathrm{pe}}] \sim \begin{cases} h_2^{\leftarrow}(b) x, & \text{for } 0 < b \leq h_2(1), \\ x, & \text{for } h_2(1) < b \leq 1, \\ b^{-1/\alpha} x, & \text{for } b > 1, \end{cases} \tag{5.13}$$

where

$$h_2(u) = u^{-\alpha} + (c_l + u)^{-\alpha} \wedge c_y - u^{-\alpha} \wedge c_y.$$

Plugging these estimates given by (5.10)–(5.13) into (5.6) and subsequently plugging the resulting estimates for HE^* into (5.7) yield two approximations for $\mathrm{BR}^{\mathrm{re}}$ and $\mathrm{BR}^{\mathrm{pe}}$. We conclude the following theorem, which represents an EVT solution to measuring the basis risk.

Theorem 5.2 *Consider* $\mathrm{BR}^{\mathrm{re}}$ *and* $\mathrm{BR}^{\mathrm{pe}}$ *defined in (5.7). Under the assumptions above, it holds for all* $0 < b \leq (c_l + 1)^{-\alpha}$ *that*

$$\lim_{x \uparrow \infty} \mathrm{BR}^{\mathrm{re}} = 1 - \frac{1 - b^{1/\alpha} h^{\leftarrow}(b)}{c_l b^{1/\alpha}} \qquad \text{and} \qquad \lim_{x \uparrow \infty} \mathrm{BR}^{\mathrm{pe}} = \frac{h^{\leftarrow}(b) - h_2^{\leftarrow}(b)}{b^{-1/\alpha} - h_2^{\leftarrow}(b)}. \tag{5.14}$$

Finally, we implement some numerical studies to check the accuracy of our asymptotic approximations for the VaR of the hedged losses and demonstrate the change of the basis risk, approximated by relation (5.14), with respect to some parameters. The choices of distributions, copulas, and related parameters are listed in Table 1.

	For $\mathrm{VaR}_q[L^{ILW}]$	For $\mathrm{VaR}_q[L^{re}]$	For $\mathrm{VaR}_q[L^{pe}]$
X	Pareto ($shape = scale = 1$)	Pareto ($shape = scale = 1$)	Pareto ($shape = scale = 1$)
Y	Pareto ($shape = 1, scale = 5$)	–	$2X$
C	Gumbel ($\gamma = 1.5$)	–	Co-monotonicity copula
c_l	2	2	2
c_y	0.5	–	0.5
$\frac{b}{(c_l+1)^{-\alpha}}$	0.9	0.9	0.9

Table 1. Parameters for checking the accuracy of asymptotic approximations (5.10), (5.12), and (5.13).

Figures 21–23 show the ratios of the asymptotic approximations for $\mathrm{VaR}_q[L^{\mathrm{ILW}}]$, $\mathrm{VaR}_q[L^{\mathrm{re}}]$, and $\mathrm{VaR}_q[L^{\mathrm{pe}}]$, given by relations (5.10)–(5.13), respectively, to the corresponding empirical estimates obtained from 10^7 samples. The ratios in Figures 21–23 all stay around 1 for reasonably large values of the attachment point x, showing that asymptotic approximations are accurate.

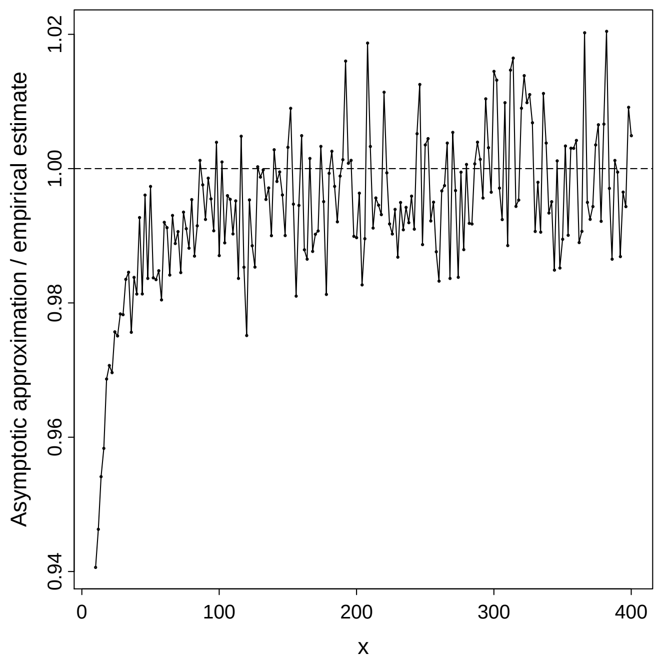

Figure 21. Accuracy of the asymptotic approximation for $\mathrm{VaR}_q\left[L^{ILW}\right]$.

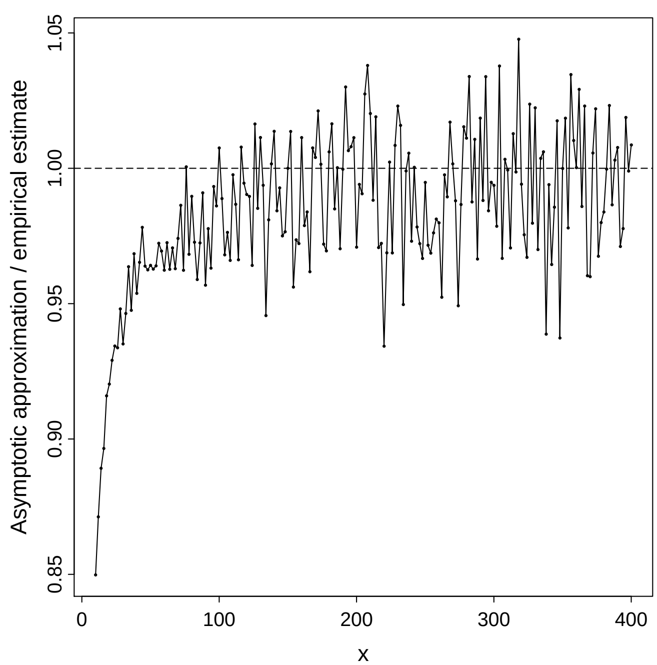

Figure 22. Accuracy of the asymptotic approximation for $\mathrm{VaR}_q\left[L^{re}\right]$.

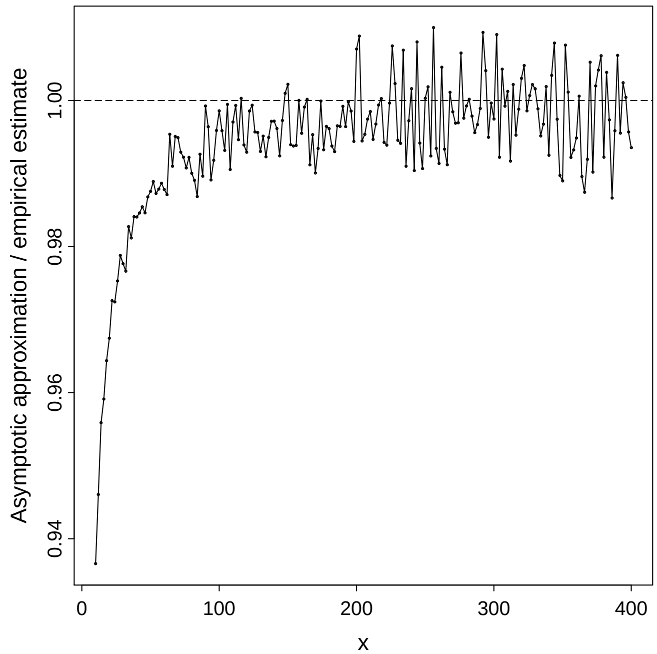

Figure 23. Accuracy of the asymptotic approximation for $\mathrm{VaR}_q\left[L^{pe}\right]$.

Figures 24–25 show the change of $\mathrm{BR}^{\mathrm{re}}$ and $\mathrm{BR}^{\mathrm{pe}}$ given by Theorem 5.2 with respect to the parameter γ of the Gumbel copula (which governs the strength of tail dependence) and the parameter c_y in (5.9). The choices of distributions, copulas, and related parameters are listed below in Table 2.

	With respect to γ	With respect to c_y
X	Pareto ($shape = 2, scale = 1$)	Pareto ($shape = 2, scale = 1$)
C	Gumbel ($\gamma \in [2, 20]$)	Gumbel ($\gamma = 2$)
x	3	3
c_l	2	2
c_y	0.5	$[0.2, 2]$
$\frac{b}{(c_l+1)^{-\alpha}}$	0.95	0.95

Table 2. Parameters for demonstrating the impact of γ, c_y, and x on the basis risk.

We see that a stronger tail dependence between the sponsor's loss X and the industry loss index Y leads to a lower basis risk. Moreover, the basis risk defined with the reinsurance being the benchmark decreases in the index trigger level y. However, the relationship is not as clear when the "perfect" ILW is used as the benchmark.

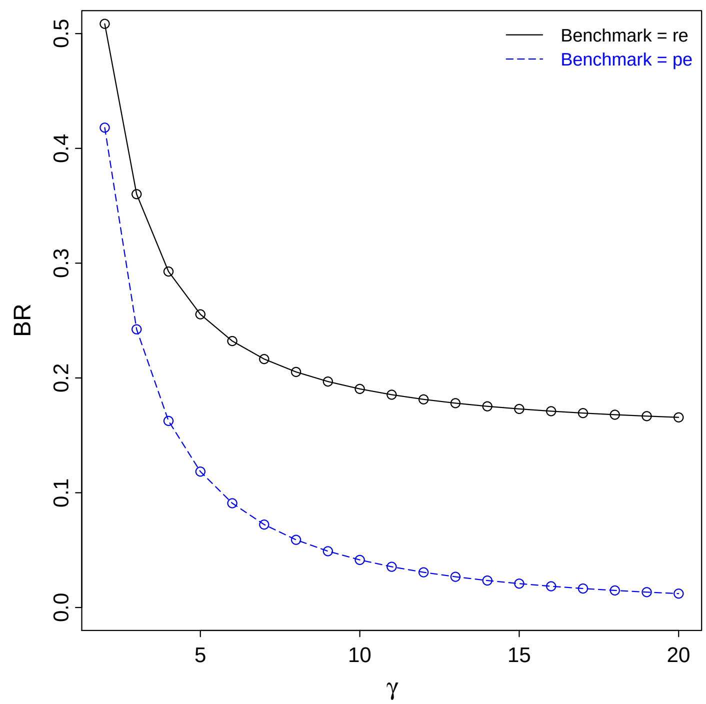

Figure 24. Change of the basis risk with respect to γ.

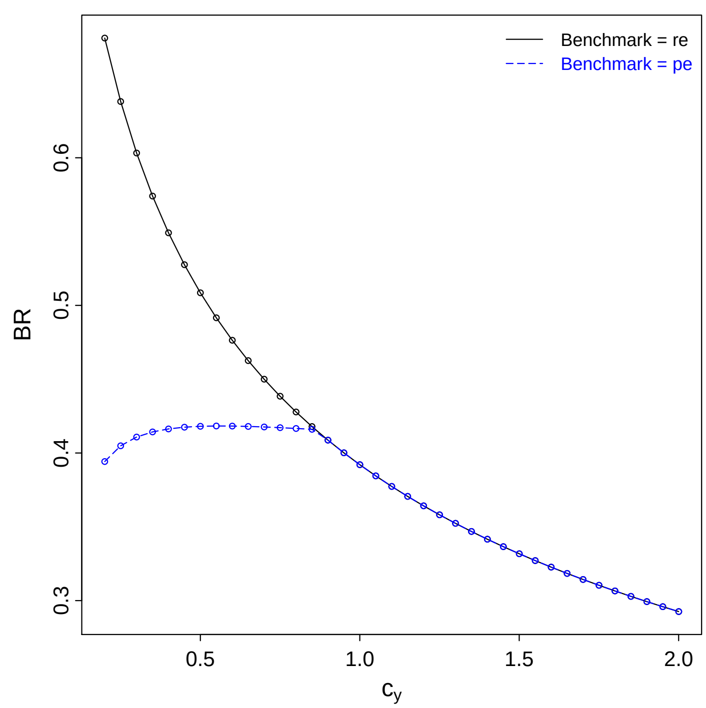

Figure 25. Change of the basis risk with respect to c_y.

6 Appendix

6.1 Proofs

Verification for Example 3.1. The verifications for (i)–(ii) are trivial. To verify (iii), denote $x = \Phi^{-1}(q)$, so that $g(q) = \Phi(x - \kappa)$ and $q = \Phi(x)$. We have

$$g'(q) = \frac{dg(q)}{dx}\frac{dx}{dq} = \frac{\Phi'(x-\kappa)}{\Phi'(x)} = e^{-\kappa^2/2}e^{\kappa x} > 0.$$

Continue this procedure to obtain

$$g''(q) = \frac{dg'(q)}{dx}\frac{dx}{dq} = \sqrt{2\pi}\kappa e^{-\kappa^2/2}e^{\frac{1}{2}x^2+\kappa x} > 0$$

and

$$g'''(q) = \frac{dg''(q)}{dx}\frac{dx}{dq} = 2\pi\kappa e^{-\kappa^2/2}e^{x^2+\kappa x}x + 2\pi\kappa^2 e^{-\kappa^2/2}e^{x^2+\kappa x} > 0.$$

We may assume by induction that

$$g^{(k)}(q) = \sum_j c_j(\kappa)e^{M_j(x)}N_j(x) > 0,$$

where the sum is taken over a finite set of j, each $M_j(x)$ and $N_j(x)$ are polynomials with non-negative (but not all zero) coefficients, and each $c_j(\kappa)$ is a positive function of κ. It is easy to verify that $g^{(k+1)}(q)$ still possesses this structure. Thus, by induction we have proven the positivity of $g^{(k)}(q)$ for all $k = 0, 1, \ldots$. ■

The following lemma will be used to establish our asymptotic estimations.

Lemma 6.1 *Suppose that $u_1 \downarrow 0$, $u_2 \downarrow 0$, and $u_1 \sim u_2$. Then it holds for every $\kappa \in \mathbb{R}$ that*

$$\overline{\Phi}\left(\Phi^{-1}(1-u_1) - \kappa\right) \sim \overline{\Phi}\left(\Phi^{-1}(1-u_2) - \kappa\right).$$

Proof. First, observe that as $x \uparrow \infty$, we have

$$\overline{\Phi}(x-\kappa) \sim \frac{\phi(x-\kappa)}{x} = \frac{\phi(x)}{x}e^{\kappa x - \kappa^2/2} \sim \overline{\Phi}(x)e^{\kappa x-\kappa^2/2},$$

where the first and last steps are due to the Mills ratio of the standard normal distribution (Mills 1926). Moreover, it is easy to verify by Lemma 6.3 of Yuan (2016) that, as $u \downarrow 0$,

$$\Phi^{-1}(1-u) = \sqrt{2\ln(1/u)} - \frac{1}{2}\ln\ln(1/u) - \frac{1}{2}\ln(4\pi) + o(1).$$

Therefore, we obtain

$$\begin{aligned} & \overline{\Phi}\left(\Phi^{-1}(1-u_1) - \kappa\right) \\ \sim\ & e^{-\kappa^2/2}u_1 \exp\left\{\kappa\Phi^{-1}(1-u_1)\right\} \end{aligned}$$

$$\begin{aligned}
&\sim \quad e^{-\kappa^2/2} u_1 \exp\left\{\kappa\left(\sqrt{2\ln(1/u_1)} - \frac{1}{2}\ln\ln(1/u_1) - \frac{1}{2}\ln(4\pi)\right)\right\} \\
&\sim \quad e^{-\kappa^2/2} u_2 \exp\left\{\kappa\left(\sqrt{2\ln(1/u_2)} - \frac{1}{2}\ln\ln(1/u_2) - \frac{1}{2}\ln(4\pi)\right)\right\} \\
&\sim \quad \overline{\Phi}\left(\Phi^{-1}(1-u_2) - \kappa\right),
\end{aligned}$$

where the third step is due to the easily verifiable fact that if two positive functions v_1 and v_2 satisfy $v_1 \to \infty$, $v_2 \to \infty$, and $v_1 \sim v_2$, then $e^{\sqrt{\ln v_1}} \sim e^{\sqrt{\ln v_2}}$. This completes the proof. ■

Proof of Proposition 4.1. For every $s \in (t, T]$, direct calculation leads to

$$\begin{aligned}
& E^{Q^1}\left[\Pi(Y_s) | Y_t = y\right] \\
= \quad & E^{Q^1}\left[\Pi(Y_{s-t} + y)\right] \\
= \quad & E^{Q^1}\left[\eta\left(F_T(Y_{s-t} + y)\right)\right] \\
= \quad & 1 - (1-c)Q^1\left(Y_{s-t} > F_T^{\leftarrow}(q_1) - y\right) - cQ^1\left(Y_{s-t} > F_T^{\leftarrow}(q_2) - y\right),
\end{aligned}$$

where in the first step we applied the fact that $\{Y_t, t \geq 0\}$ is a homogeneous Markov process and in the last two steps we applied relations (4.4)–(4.5). Thus,

$$E^{Q^1}\left[\Pi(Y_s) | Y_t = y\right] = 1 - (1-c)\overline{\Phi}\left(\Phi^{\leftarrow}(1-p_1) - \kappa\right) - c\overline{\Phi}\left(\Phi^{\leftarrow}(1-p_2) - \kappa\right) \tag{6.1}$$

with $p_j = P^1\left(Y_{s-t} > F_T^{\leftarrow}(q_j) - y\right)$, $j = 1, 2$. Note that we have

$$P^1\left(Y_{s-t} > x\right) \sim \lambda(s-t)\mu(A)\overline{F}(x), \qquad x \to \infty,$$

and

$$F_T^{\leftarrow}(q_j) \sim F^{\leftarrow}\left(1 - \frac{1-q_j}{\lambda T \nu(A)}\right), \qquad q_j \uparrow 1.$$

It follows that

$$p_j \sim \lambda(s-t)\nu(A)\overline{F}\left(F^{\leftarrow}\left(1 - \frac{1-q_j}{\lambda T\nu(A)}\right) - y\right), \qquad q_j \uparrow 1. \tag{6.2}$$

By Lemma 6.1, plugging (6.2) into (6.1) yields the desired result in (4.7). ■

Proof of Lemma 5.1. It is easy to verify that

$$\left(L^{\text{ILW}} > z\right) = \begin{cases} (X > l + z, Y > y) \cup (X > z, Y \leq y), & \text{for } z \geq x, \\ (X > z), & \text{for } z < x. \end{cases}$$

For $u \geq 1$, it follows that

$$P\left(L^{\text{ILW}} > ux\right) = P\left(X > l + ux, Y > y\right) + P\left(X > ux, Y \leq y\right).$$

For the the first probability on the right-hand side, notice that

$$P\left(X > l + ux, Y > y\right) = \hat{C}\left(\overline{F}(l + ux), \overline{G}(y)\right).$$

Our assumptions $l/x \to c_l$ and $\overline{G}(y)/\overline{F}(x) \to c_y$ in (5.9) as well as $\overline{F} \in \mathrm{RV}_{-\alpha}$ imply that, for arbitrarily fixed $0 < \varepsilon < 1$ and all large x,

$$\begin{aligned} & \hat{C}\left((1-\varepsilon)(c_l+u)^{-\alpha}\overline{F}(x), (1-\varepsilon)c_y\overline{F}(x)\right) \\ \leq\ & \hat{C}\left(\overline{F}(l+ux), \overline{G}(y)\right) \\ \leq\ & \hat{C}\left((1+\varepsilon)(c_l+u)^{-\alpha}\overline{F}(x), (1+\varepsilon)c_y\overline{F}(x)\right). \end{aligned}$$

Applying relation (5.8) to both sides yields that

$$\begin{aligned} & H\left((1-\varepsilon)(c_l+u)^{-\alpha}, (1-\varepsilon)c_y\right)\overline{F}(x) \\ \lesssim\ & \hat{C}\left(\overline{F}(l+ux), \overline{G}(y)\right) \\ \lesssim\ & H\left((1+\varepsilon)(c_l+u)^{-\alpha}, (1+\varepsilon)c_y\right)\overline{F}(x). \end{aligned}$$

By the continuity of the bivariate function H, we obtain

$$\hat{C}\left(\overline{F}(l+ux), \overline{G}(y)\right) \sim H\left((c_l+u)^{-\alpha}, c_y\right)\overline{F}(x).$$

Hence,

$$P\left(X > l+ux, Y > y\right) \sim H\left((c_l+u)^{-\alpha}, c_y\right)\overline{F}(x).$$

For the second probability, we derive

$$\begin{aligned} P\left(X > ux, Y \leq y\right) &= P\left(X > ux\right) - P\left(X > ux, Y > y\right) \\ &= \overline{F}(ux) - \hat{C}\left(\overline{F}(ux), \overline{G}(y)\right) \\ &\sim u^{-\alpha}\overline{F}(x) - H\left(u^{-\alpha}, c_y\right)\overline{F}(x). \end{aligned}$$

For $0 < u < 1$, straightforwardly,

$$P\left(L^{\mathrm{ILW}} > ux\right) = P\left(X > ux\right) \sim u^{-\alpha}\overline{F}(x).$$

Therefore,

$$\lim_{x\to\infty} \frac{P\left(L^{\mathrm{ILW}} > ux\right)}{\overline{F}(x)} = \begin{cases} h(u), & \text{for } u \geq 1, \\ u^{-\alpha}, & \text{for } 0 < u < 1, \end{cases} \tag{6.3}$$

where the function $h(u)$ is given by relation (5.11). Note that the right-hand side of (6.3) as a function of u has a jump at 1 and is continuous elsewhere. The three relations in (5.10) are then obtained by inverting the right-hand side of (6.3) accordingly. This completes the proof. ■

Proof of Theorem 5.2. First, notice that both $h(u)$ and $h_2(u)$ decrease to $h_1(u)$ as $c_y \uparrow \infty$, which implies that $h_1(u) \leq \min\{h(u), h_2(u)\}$ for $u > 0$. Thus, for $0 \leq b \leq h_1(1) = (c_l+1)^{-\alpha}$, the first relations in (5.10)–(5.13) apply. It follows straightforwardly that

$$\mathrm{BR}^{\mathrm{re}} = 1 - \frac{\mathrm{HE}^{\mathrm{ILW}}}{\mathrm{HE}^{\mathrm{re}}}$$

$$
\begin{aligned}
&= 1 - \frac{\mathrm{VaR}_q[X] - \mathrm{VaR}_q\left[L^{\mathrm{ILW}}\right]}{\mathrm{VaR}_q[X] - \mathrm{VaR}_q[L^{\mathrm{re}}]} \\
&\to 1 - \frac{b^{-1/\alpha}x - h^{\leftarrow}(b)x}{b^{-1/\alpha}x - \left(b^{-1/\alpha} - c_l\right)x} \\
&= 1 - \frac{1 - b^{1/\alpha}h^{\leftarrow}(b)}{c_l b^{1/\alpha}}.
\end{aligned}
$$

Similarly,

$$
\begin{aligned}
\mathrm{BR}^{\mathrm{pe}} &= 1 - \frac{\mathrm{HE}^{\mathrm{ILW}}}{\mathrm{HE}^{\mathrm{pe}}} \\
&= \frac{\mathrm{VaR}_q\left[L^{\mathrm{ILW}}\right] - \mathrm{VaR}_q[L^{\mathrm{pe}}]}{\mathrm{VaR}_q[X] - \mathrm{VaR}_q[L^{\mathrm{pe}}]} \\
&\to \frac{h^{\leftarrow}(b) - h_2^{\leftarrow}(b)}{b^{-1/\alpha} - h_2^{\leftarrow}(b)}.
\end{aligned}
$$

This completes the proof. ■

6.2 Illustration of the block maxima method

As an example, assume that in year s, the day j earthquake magnitude in the specified region is $\Theta_{s,j}$, and that $\{\Theta_{s,j}, s = 1, \ldots, T,\ j = 1, \ldots, 365\}$ are i.i.d. random variables with generic random variable Θ and common distribution in $\mathrm{MDA}(H_\xi)$. If Y_s is the maximum magnitude of the earthquakes by year s, that is,

$$
Y_s = \max_{1 \le k \le s, 1 \le j \le 365} \Theta_{k,j},
$$

then we may use the block maxima method to approximate the distribution of Y_s. Recall that coupon payments are made every year, and, hence, for $t \in [0, T]$, we need to approximate, for every year s, $s = 1, \ldots, T$, the conditional distribution function of $Y_s |\, Y_t = y$, which is identical in distribution to $Y_{s-t} \vee y$.

Rewrite

$$
Y_s = \max_{1 \le k \le s} \max_{1 \le j \le 365} \Theta_{k,j} = \max_{1 \le k \le s} M_k.
$$

By the definition of $\mathrm{MDA}(H_\xi)$, there are constants $c > 0$ and $d \in \mathbb{R}$ such that the distribution of $(M_k - d)/c$ is approximately $H_\xi(x)$, or, equivalently,

$$
P^1 (M_k \le x) \approx \exp\left\{-(1 + \xi(cx + d))^{-1/\xi}\right\}.
$$

Standard statistical methods (such as maximum likelihood estimation) are available to obtain estimates $\hat{c}$, $\hat{d}$, and $\hat{\xi}$ for the parameters above. As a result, we have, for $x \ge y$,

$$
\begin{aligned}
& P^1 (Y_s \le x |\, Y_t = y) \\
=\ & P^1 (Y_{s-t} \vee y \le x) \\
\approx\ & \exp\left\{-(s - t)(1 + \hat{\xi}(\hat{c}x + \hat{d}))^{-1/\hat{\xi}}\right\},
\end{aligned}
$$

and for $x < y$ it is equal to 0.

6.3 Interest rate models

Throughout the report, we model, under the risk-neutral measure Q^2, the annualized instantaneous risk-free interest rate process $\{r_t, t \geq 0\}$ by a Cox–Ingersoll–Ross (CIR) model (see Cox et al. 1985):

$$dr_t = a_r (b_r - r_t)\, dt + \sigma_r \sqrt{r_t} dW_{r,t}, \tag{6.4}$$

where a_r, b_r, and σ_r are positive numbers, with a_r corresponding to the speed of mean reversion, b_r the long-run mean, and σ_r the volatility, and $W_{r,t}$ a standard Brownian motion under Q^2. The CIR process is clearly a time-homogeneous Markov process, and it is known that if $2a_r b_r \geq \sigma_r^2$, then the positivity of r_t is guaranteed. Also, under such a process for the short rate, we have

$$E^{Q^2}[D(0,t)] = A(0,t)e^{-B(0,t)r_0}, \qquad t \geq 0, \tag{6.5}$$

where

$$\begin{aligned}
A(0,t) &= \left(\frac{2he^{(a_r+h)t/2}}{2h + (a_r+h)(e^{th}-1)} \right)^{2a_r b_r/\sigma_r^2}, \\
B(0,t) &= \frac{2\left(e^{th}-1\right)}{2h + (a_r+h)(e^{th}-1)}, \\
h &= \sqrt{a_r^2 + 2\sigma_r^2}.
\end{aligned}$$

By the time-homogeneity property, we have, for $s \geq t \geq 0$,

$$E_t^{Q^2}[D(t,s)] = A(0,s-t)e^{-B(0,s-t)r_t}.$$

Moreover, as stated in Subsection 4.1, we consider a continuous-time LIBOR process $\{\ell_t, t \geq 0\}$ and let the floating coupon rate be $i_t = \ell_t$ for $t \in \mathbb{N}$. We assume that under Q^2 the LIBOR $\{\ell_t, t \geq 0\}$ follows another CIR process,

$$d\ell_t = a_\ell (b_\ell - \ell_t)\, dt + \sigma_\ell \sqrt{\ell_t} dW_{\ell,t}, \qquad t \geq 0, \tag{6.6}$$

where a_ℓ, b_ℓ, and σ_ℓ are positive numbers interpreted similarly to the above, and $W_{\ell,t}$ is another standard Brownian motion under Q^2, satisfying

$$dW_{r,t} dW_{\ell,t} = \rho dt, \qquad t \geq 0,$$

for some $\rho \in (-1, 1)$. Putting the two processes together, we see that the bivariate stochastic process $\{(r_t, \ell_t), t \geq 0\}$ forms a special case of the affine term structure model (9) of Dai and Singleton (2000) and, in particular, is a time-homogeneous Markov process.

We use simulation to estimate the term $E_t^{Q^2}[D(t,s)\ell_s]$ in relation (3.6). The simulation of CIR processes is known to be a challenging problem and has been discussed extensively in the literature under the more general framework of the Heston stochastic volatility models; see Heston (1993) for the introduction of the Heston models and see, for example, Andersen (2008) and Alfonsi (2010) for discussions of simulations of these processes. Generally, two kinds of methods can be used for this simulation, discretization methods and exact simulation methods, both subject to criticisms. Discretization methods such as the Euler–Maruyama method may introduce bias that is not easy to reduce, and exact simulation methods require exact knowledge about the conditional distributions of the underlying process, which is a problem, especially in a multivariate case like what we need to handle here. We follow a discretization method proposed by Lord et al. (2010), the so-called full truncation method. The method has been proven by the authors to produce discretization that leads to strongly converging approximations. To estimate $E_t^{Q^2}[D(t,s)\ell_s]$, we use this method to generate 10^5 paths for both CIR processes.

Acknowledgments: This project was supported by a research grant (2014–2016) from the Society of Actuaries entitled "Modeling and Analyzing Extreme Risks in Insurance." The authors would like to thank Project Oversight Group members Jim Berger, Tom Edwalds, Robert Reitano, and David Wylde for their constructive comments on the report, and we thank Jan Schuh and Ronora Stryker for their excellent coordination and great help during the whole process of this project. They also acknowledge the California Department of Conservation's California Geological Survey for making available the California earthquake catalog used in Section 4.1.

References

[1] Alfonsi, A. High order discretization schemes for the CIR process: application to affine term structure and Heston models. *Mathematics of Computation* 79 (2010), 209–237.

[2] Andersen, L. Simple and efficient simulation of the Heston stochastic volatility model. *Journal of Computational Finance* 11 (2008), 1–42.

[3] Bali, T. G. An extreme value approach to estimating interest-rate volatility: pricing implications for interest-rate options. *Management Science* 53 (2007), 323–339.

[4] Barrieu, P., Loubergé, H. Hybrid cat bonds. *Journal of Risk and Insurance* 76 (2009), 547–578.

[5] Beirlant, J., Goegebeur, Y., Teugels, J., Segers, J. *Statistics of Extremes. Theory and Applications.* John Wiley & Sons, Chichester, 2004.

[6] Bingham, N. H., Goldie, C. M., Teugels, J. L. *Regular Variation.* Cambridge University Press, Cambridge, 1987.

[7] Björk, T. *Arbitrage Theory in Continuous Time.* Oxford University Press, Oxford, 2009.

[8] Cox, S. H., Fairchild, J. R., Pedersen, H. W. Economic aspects of securitization of risk. *ASTIN Bulletin* 30 (2000), 157–193.

[9] Cox, J. C., Ingersoll Jr., J. E., Ross, S. A. A theory of the term structure of interest rates. *Econometrica* 53 (1985), 385–407.

[10] Cox, S. H., Pedersen, H. W. Catastrophe risk bonds. *North American Actuarial Journal* 4 (2000), 56–82.

[11] Cummins, J. D. CAT bonds and other risk-linked securities: state of the market and recent developments. *Risk Management and Insurance Review* 11 (2008), 23–47.

[12] Cummins, J. D., Lalonde, D., Phillips, R. D. The basis risk of catastrophic-loss index securities. *Journal of Financial Economics* 71 (2004), 77–111.

[13] Cummins, J. D., Weiss, M. A. Convergence of insurance and financial markets: hybrid and securitized risk-transfer solutions. *Journal of Risk and Insurance* 76 (2009), 493–545.

[14] Dai, Q., Singleton, K. J. Specification analysis of affine term structure models. *Journal of Finance* 55 (2000), 1943–1978.

[15] de Haan, L., Ferreira, A. *Extreme Value Theory: An Introduction*. Springer, New York, 2006.

[16] Denneberg, D. *Non-additive Measure and Integral*. Springer Science & Business Media, New York, 1994.

[17] Di Bernardino, E., Rullière, D. Distortions of multivariate distribution functions and associated level curves: applications in multivariate risk theory. *Insurance: Mathematics and Economics* 53 (2013), 190–205.

[18] Donnelly, C., Embrechts, P. The devil is in the tails: actuarial mathematics and the subprime mortgage crisis. *ASTIN Bulletin* 40 (2010), 1–33.

[19] Dubinsky, W., Laster, D. Insurance-linked securities. Swiss Re Capital Markets Corporation, 2003.

[20] Egami, M., Young, V. R. Indifference prices of structured catastrophe (CAT) bonds. *Insurance: Mathematics and Economics* 42 (2008), 771–778.

[21] Embrechts, P., Klüppelberg, C., Mikosch, T. *Modelling Extremal Events for Insurance and Finance*. Springer, Berlin, 1997.

[22] Embrechts, P., Resnick, S. I., Samorodnitsky, G. Living on the edge. *Risk* 11 (1998), 96–100.

[23] Embrechts, P., Resnick, S. I., Samorodnitsky, G. Extreme value theory as a risk management tool. *North American Actuarial Journal* 3 (1999), 30–41.

[24] Galeotti, M., Gürtler, M., Winkelvos, C. Accuracy of premium calculation models for CAT bonds—an empirical analysis. *Journal of Risk and Insurance* 80 (2013), 401–421.

[25] Gatzert, N., Kellner, R. The influence of nonlinear dependencies on the basis risk of industry loss warranties. *Insurance: Mathematics and Economics* 49 (2011), 132–144.

[26] Gürtler, M., Hibbeln, M., Winkelvos, C. The impact of the financial crisis and natural catastrophes on CAT bonds. *Journal of Risk and Insurance* 83 (2016), 579–612.

[27] Guy Carpenter & Company. *The Catastrophe Bond Market at Year-end 2006*. Guy Carpenter & Company, New York, 2007.

[28] Heston, S. L. A closed-form solution for options with stochastic volatility with applications to bond and currency options. *Review of Financial Studies* 6 (1993), 327–343.

[29] Jaworski, P. On uniform tail expansions of bivariate copulas. *Applicationes Mathematicae (Warsaw)* 31 (2004), 397–415.

[30] Joe, H., Li, H., Nikoloulopoulos, A. K. Tail dependence functions and vine copulas. *Journal of Multivariate Analysis* 101 (2010), 252–270.

[31] Kellner, R., Gatzert, N. Estimating the basis risk of index-linked hedging strategies using multivariate extreme value theory. *Journal of Banking & Finance* 37 (2013), 4353–4367.

[32] Kelly, B., Jiang, H. Tail risk and asset prices. *Review of Financial Studies* 27 (2014), 2841–2871.

[33] Lane, M. N., Beckwith R. G. The annual 2009 ILS review—and Q1 2009 quarterly performance review: change we can believe in. Lane Financial LLC Trade Notes, 2009.

[34] Lee, J., Yu, M. Pricing default-risky CAT bonds with moral hazard and basis risk. *Journal of Risk and Insurance* 69 (2002), 25–44.

[35] Leobacher, G., Ngare, P. Utility indifference pricing of derivatives written on industrial loss indices. *Journal of Computational and Applied Mathematics* 300 (2016), 68–82.

[36] Li, H., Sun, Y. Tail dependence for heavy-tailed scale mixtures of multivariate distributions. *Journal of Applied Probability* 46 (2009), 925–937.

[37] Lin, Y., Cox, S. H. Securitization of catastrophe mortality risks. *Insurance: Mathematics and Economics* 42 (2008), 628–637.

[38] Lord, R., Koekkoek, R., Dijk, D. V. A comparison of biased simulation schemes for stochastic volatility models. *Quantitative Finance* 10 (2010), 177–194.

[39] Ma, Z., Ma, C. Pricing catastrophe risk bonds: a mixed approximation method. *Insurance: Mathematics and Economics* 52 (2013), 243–254.

[40] McDonnell, E. Industry loss warranties. In *Alternative Risk Strategies,* edited by M. Lane. Risk Books, London, 2002.

[41] McNeil, A. J., Frey, R. Estimation of tail-related risk measures for heteroscedastic financial time series: an extreme value approach. *Journal of Empirical Finance* 7 (2000): 271–300.

[42] McNeil, A. J., Frey, R., Embrechts, P. *Quantitative Risk Management. Concepts, Techniques and Tools* (revised edition). Princeton University Press, Princeton, NJ, 2015.

[43] Mills, J. P. Table of the ratio: area to bounding ordinate, for any portion of normal curve. *Biometrika* 18 (1926), 395–400.

[44] Mitra, A., Resnick, S. I. Hidden regular variation and detection of hidden risks. *Stochastic Models* 27 (2011), 591–614.

[45] Muermann, A. Market price of insurance risk implied by catastrophe derivatives. *North American Actuarial Journal* 12 (2008), 221–227.

[46] National Association of Insurance Commissioners (NAIC). A comprehensive overview of the insurance-Linked securities market. Technical Report (2012).

[47] Nelsen, R. B. *An Introduction to Copulas.* Springer Science & Business Media, New York, 2006.

[48] Nowak, P., Romaniuk, M. Pricing and simulations of catastrophe bonds. *Insurance: Mathematics and Economics* 52 (2013), 18–28.

[49] Øksendal, B. *Stochastic Differential Equations* (6th edition). Springer-Verlag, Berlin, 2003.

[50] Resnick, S. I. *Heavy-Tail Phenomena. Probabilistic and Statistical Modeling.* Springer, New York, 2007.

[51] Ross, D., Williams, J. Basis risk from the cedant's perspective. In *The Handbook of Insurance-Linked Securities,* edited by P. Barrieu and L. Albertini. John Wiley & Sons, New York, 2009.

[52] Shao, J., Pantelous, A., Papaioannou, A. D. Catastrophe risk bonds with applications to earthquakes. *European Actuarial Journal* 5 (2015), 113–138.

[53] Tang, Q., Yuan, Z. Asymptotic analysis of the loss given default in the presence of multivariate regular variation. *North American Actuarial Journal* 17 (2013), 253–271.

[54] van Oordt, M. R. C., Zhou, C. Systematic tail risk. *Journal of Financial and Quantitative Analysis* 51 (2016), 685–705.

[55] Wang, S. Premium calculation by transforming the layer premium density. *ASTIN Bulletin* 26 (1996), 71–92.

[56] Wang, S. A class of distortion operators for pricing financial and insurance risks. *Journal of Risk and Insurance* 67 (2000), 15–36.

[57] Wang, S. A universal framework for pricing financial and insurance risks. *ASTIN Bulletin* 32 (2002), 213–234.

[58] Wang, S. CAT bond pricing using probability transforms. *Geneva Papers: Etudes et Dossiers* 278 (2004), 19–29.

[59] Yuan, Z. An asymptotic characterization of hidden tail credit risk with actuarial applications. Preprint (2016).

[60] Zeng, L. On the basis risk of industry loss warranties. *Journal of Risk Finance* 1 (2000), 27–32.

[61] Zimbidis, A. A., Frangos, N. E., Pantelous A. A. Modeling earthquake risk via extreme value theory and pricing the respective catastrophe bonds. *ASTIN Bulletin* 37 (2007), 163–183.